Traumatic events in the life of the deep-sea cephalopod mollusc, the coleoid Spirula spirula

Hoffmann, R ; Lemanis, R E ; Wulff, L ; Zachow, S ; Lukeneder, A ; Klug, C ; Keupp, H

Abstract: Here, we report on different types of shell pathologies of the enigmatic deep-sea (mesopelagic) cephalopod Spirula spirula. For the first time, we apply non-invasive imaging methods to: document trauma-induced changes in shell shapes, reconstruct the different causes and effects of these pathologies, unravel the etiology, and attempt to quantify the efficiency of the buoyancy apparatus. We have analysed 2D and 3D shell parameters from eleven shells collected as beach findings from the Canary Islands (Gran Canaria and Fuerteventura), West-Australia, and the Maldives. All shells were scanned with a nanotom-m computer tomograph. Seven shells were likely injured by predator attacks: fishes, cephalopods or crustaceans, one specimen was infested by an endoparasite (potentially Digenea) and one shell shows signs of inflammation and one shell shows large fluctuations of chamber volumes without any signs of pathology. These fluctuations are potential indicators of a stressed environment. Pathological shells represent the most deviant morphologies of a single species and can therefore be regarded as morphological end-members. The changes in the shell volume / chamber volume ratio were assessed in order to evaluate the functional tolerance of the buoyancy apparatus showing that these had little effect. Key words: pathology; parasitism; Spirula; mesopelagic; ecology; predator; buoyancy; cephalopods

DOI: https://doi.org/10.1016/j.dsr.2018.10.007

Traumatic events in the life of the deep-sea cephalopod mollusc, the coleoid *Spirula spirula*

R. Hoffmann, R.E. Lemanis, L. Wulff, S. Zachow, A. Lukeneder, C. Klug, H. Keupp

PII: S0967-0637(18)30145-6
DOI: https://doi.org/10.1016/j.dsr.2018.10.007
Reference: DSRI2973

To appear in: *Deep-Sea Research Part I*

Received date: 7 May 2018
Revised date: 18 October 2018
Accepted date: 20 October 2018

Cite this article as: R. Hoffmann, R.E. Lemanis, L. Wulff, S. Zachow, A. Lukeneder, C. Klug and H. Keupp, Traumatic events in the life of the deep-sea cephalopod mollusc, the coleoid *Spirula spirula*, *Deep-Sea Research Part I,* https://doi.org/10.1016/j.dsr.2018.10.007

Traumatic events in the life of the deep-sea cephalopod mollusc, the coleoid *Spirula spirula*

Hoffmann, R.[a,*,1], Lemanis, R. E.[b], Wulff, L.[a], Zachow, S.[c], Lukeneder, A.[d], Klug, C.[e] and Keupp, H.[f]

[a] Institute of Geology, Mineralogy & Geophysics, Ruhr-Universität Bochum, Bochum, 44801, Germany

[b] B CUBE – Center for Molecular Bioengineering, Technische Universität Dresden, Dresden, 01307, Germany

[c]Division of Mathematics for Life and Materials Sciences, Department of Visual Data Analysis, Zuse Institute Berlin (ZIB), Berlin, 14195, Germany

[d] Geological-Palaeontological Department, Natural History Museum, 1010 Vienna, Austria

[e] Paläontologisches Institut und Museum, University of Zurich, Zurich, Switzerland

[f] Section Palaeontology, Institute of Earth Sciences, Freie Universität Berlin, Berlin, Germany

[*]Corresponding author: rene.hoffmann@rub.de

Abstract:

Here, we report on different types of shell pathologies of the enigmatic deep-sea (mesopelagic) cephalopod *Spirula spirula.* For the first time, we apply non-invasive imaging methods to: document trauma-induced changes in shell shapes, reconstruct the different causes and effects of these pathologies, unravel the etiology, and attempt to quantify the efficiency of the buoyancy apparatus. We have analysed 2D and 3D shell parameters from eleven shells collected as beach findings from the Canary Islands (Gran Canaria and Fuerteventura), West-Australia, and the Maldives. All shells were scanned with a nanotom-m computer tomograph. Seven shells were likely injured by predator attacks: fishes, cephalopods or crustaceans, one specimen was infested by an endoparasite (potentially Digenea) and one shell shows signs of inflammation and one shell shows large fluctuations of chamber volumes without any signs of pathology. These fluctuations are potential indicators of a stressed environment. Pathological shells represent the most deviant morphologies of a single species and can therefore be regarded as morphological end-members. The changes in the shell volume / chamber volume ratio were assessed in order to evaluate the functional tolerance of the buoyancy apparatus showing that these had little effect.

[1] ORCID-ID: 0000-0001-7992-1264

Key words:
pathology; parasitism; Spirula; mesopelagic; ecology; predator; buoyancy; cephalopods

1 Introduction

Pathological phenomena (syndromes) of mineralized hardparts (e.g., bones or shells) represent a unique source of information that can help to understand the ecology or life modes of organisms that are either difficult to observe in their natural habitat or extinct. Pathologies can have a syn- or autecological, i.e. external or internal, origin (Keupp 1984, 1985). Synecology refers to the interaction between different species, e.g. predator-prey-relationships, parasitism, or epizoism, while autecology refers to the interactions of an organism with its environment. These specific types of interactions will result in characteristic reactions of the involved organisms and can lead to typical anomalous growth patterns (e.g., Conway Morris 1981, Halstead 1990, Keupp 2012, De Baets et al. 2015b, Hoffmann and Keupp 2015). In this context, it is important to note that the resulting degree of anomalous growth always ranges within specific tolerance limits and allows estimating the functional tolerance of distinct morphological traits. Independent of this, these pathological shells are regarded as morphological end-members when exploring the potential intraspecific variability of distinct species (e.g., De Baets et al. 2015a, Stilkerich et al. 2017).

The majority of pathological and palaeo-pathological studies focus on vertebrates (e.g., Tasnadi-Kubacska 1962; Pinhasi and Mays 2007; Grauer 2012). In the past decades, modern and fossil cephalopods with pathological or teratological deformations have received increasing attention (Hölder 1956; Guex 1967; Kabanov 1967; Keupp 1973, 2000, 2002, 2012; Ward and Boletzky 1984; Boletzky and Overath 1989; Hochberg 1990; Hanlon and Forsythe 1990; Hengsbach 1996; Pascual et al. 1996, 2007; Gestal et al. 1999; Kröger 2000; Bello and Paparella 2003; González et al. 2003; Klug 2007; Castellanos-Martínez and Gestal 2013; Keupp and Fuchs 2014, De Baets et al. 2015b, Hoffmann et al. 2018, Imperadore and Fiorito 2018).

Cephalopods are a commonly studied group in both biology and palaeontology, largely due to their long phylogenetic history that starts in the Cambrian (Kröger et al. 2011), a global distribution and high abundances in both modern oceans and in the fossil record (e.g., ammonoids), and their importance for commercial fisheries (e.g., Rodhouse et al. 2014). Mollusc shells share a great advantage in the study of pathologies due to the accretionary

growth of their shells, which bear an ontogenetic record of the effects of the pathology and the animal's response.

Only three modern cephalopod groups retain a mineralized (aragonitic), chambered shell, i.e. nautiloids (*Nautilus*, *Allonautilus*), sepiids (e.g. *Sepia*), and *Spirula spirula.* These groups have often been used as modern analogues of the extinct ammonoids (417-65 Ma) due to similarities in their shell mineralogy, morphology, and assumed similar function of the chambered shell (Appellöf 1893; Prell 1921; Mutvei 1964, 2016; Dauphin 1976; Warnke and Keupp 2005; Klug et al. 2008; Yamaguchi et al. 2015; Klug and Hoffmann 2015). For example, the internal shell of *Spirula spirula* is loosely coiled resembling the shell morphologies of Early Devonian and some Cretaceous (heteromorphs) ammonoids (Stilkerich et al. 2017). That resemblance is superficial due to the endogastric coiling of *Spirula* while externally shelled heteromorph ammonoids have an exogastric coiled shell.

Ecological information about the deep-sea cephalopods, as for all deep-sea creatures, are scarce. Major contributions to the understanding of the *Spirula* animal date back to Huxley and Pelseneer (1895), Chun (1910, 1915), Kerr (1931), Bruun (1943, 1955), and Clarke (1969, 1970) and have been reviewed by Hoffmann and Warnke (2014). *Spirula* is well known for its daily vertical migrations, spending the daytime around depths of about 600-700 m) and the night around depths of 100-300 m (Clarke 1969). Because live caught specimens are rare, recent attempts used the $\delta^{18}O$ signal of their aragonitic shell to decipher, e.g, vertical ontogenetic migration patterns (Lukeneder et al. 2008; Price et al. 2009; Warnke et al. 2010). Vertical migration can be achieved by using the jet as well as the two fins while predominantly hanging head-down in the water column (Hoffmann and Warnke 2014). For its orientation in the water column *Spirula* possesses two Statoliths – which are the only carbonatic mineralized hard parts besides the shell. Both statoliths lie within a liquid filled statocyste near to the brain. Clarke (1978) reported on 12-13 mm^3 large disc-shaped statoliths for adult *Spirula*. Based on size distribution within a population, Clarke (1970) and Nesis (1987) speculated about the life span of *Spirula* ranging between 12-20 months, which is similar to the majority of coleoids. *Spirula* feeds on pelagic crustaceans such as copepods, ostracods but also euphausids, mysids, and small decapods (Nixon and Dilly 1977, Young 1977, Ballantine et al. 1981). Recent analysis of nitrogen isotopes of the *Spirula* shell carbonate largely supports earlier findings regarding *Spirula* as a detritus and zooplankton feeding animal (Ohkouchi et al. 2013). In *Spirula*, modern nautiloids and sepiids, the mineralized shell acts as a buoyancy device where the liquid in every newly formed chamber is removed through the siphuncle (Mutvei 2016). The chambers of *Spirula* and *Nautilus* were

filled with a gas, enriched in nitrogen, which was extracted from the blood in the siphuncle to make the animal neutrally buoyant (Denton et al. 1967; Denton and Gilpin-Brown 1971). We assume that the growth of shell and soft tissues, as well as the formation of new chambers are strictly synchronous. Pathologies, including loss but also addition of shell material, allow for an assessment of the functional tolerance of this buoyancy apparatus (Ward 1987; Keupp 2000; Kröger 2000; Klug and Hoffmann 2015; Hoffmann et al. 2015).

Studies of pathological shell-bearing cephalopods are largely restricted to surface evaluations due to reluctance to damage such rare materials (with one exception, where an ammonoid was serial sectioned, revealing deformations of the phragmocone: Tajika et al. 2015). Few pathological fossil cephalopods have been analyzed with non-invasive imaging techniques such as computed tomography (Keupp and Mitta 2004; Gonzalez et al. 2017; Stilkerich et al. 2017), or magnetic resonance imaging (Mietchen et al. 2005, 2008; Hoffmann et al. 2014; Giovanetti et al. 2016). The examination of pathologies however, often remains purely descriptive and highly speculative. Based on high-resolution computed tomography (CT) data, we assess pathological shells of the enigmatic deep-sea coleoid *Spirula spirula.* In the first report on pathological *Spirula* shells, Keupp (2012) refers to endogenic reasons (autecologic) for the malformation of the initial chamber (protoconch), which is normally spherical, or the secretion of additional shell material forming a callus-like structure at the preserved shell margin.

The aims of our study are (i) to give a detailed description of the pathological phenomena and the ontogenetic timing of the different types of phenomena, (ii) to identify the potential origin (etiology) of these pathologies, (iii) to quantify the effect of these pathologies on shell morphology and to explore the corresponding limits of intraspecific variability, and (iv) to explore the functional tolerance of the buoyancy apparatus in *Spirula*.

2 Material and methods

We examined 11 specimens of the extant deep-sea cephalopod *Spirula spirula* (Spirulidae, Decabrachia, Coleoidea see Sanchez et al. 2018). Eight shells were collected on beaches on Fuerteventura and Gran Canaria (Canary Islands) while one live specimen was caught off Northwest Africa. One shell was found on West-Australia and one on the Maldives. Collected 2D- and 3D data of the newly acquired shells are compared with data of a single shell from Fuerteventura published in Hoffmann et al. (2015a). We selected the shells from the Canary Islands and West-Australia, newly described herein, due to obvious shell anomalies. Three of the shells from Gran Canaria had been described earlier by Keupp (2012) and are now housed

at the Bayerische Staatssammlung Munich (Germany) with the coll. no. SHK PC-5 / BSPG 2014 XXI 88005 (blister), illustrated in Keupp (2012, p. 347, fig. 436), SHK PC-6 / BSPG 2014 XXI 88006 (callus), figured in Keupp (2012, p. 346, fig. 435 top), and SHK PC-7 / BSPG 2014 XXI 88007 (callus), displayed in Keupp (2012, p. 346, fig. 435 bottom); all of these specimens were collected by G. Moschner (1/2007). Two additional shells were found on Gran Canaria (leg. Dr. U. Schneider geb. Nützel), SNSB-BSPG 2018 I 21 and -22. The shell from W-Australia is deposited at the Natural History Museum Vienna (Austria) coll. no. 2015/0020/0007. We chose the shell from the Maldives as a "normal" shell to compare it with pathological shells; it is also deposited at the Natural History Museum Vienna (Austria) with the coll. no. 2015/0022/0001. Furthermore, we used a live caught specimen to assess the soft body to shell volume ratio. All shells have been scanned with a nanotom-m computer tomograph at iWP (Neuss, Germany, Table 1).

Because *Spirula* shells resemble those of Devonian and Cretaceous heteromorph ammonoids, the description of conch geometry largely follows standard ammonite terminology Korn and Klug (2007), De Baets et al. (2009, 2013, 2015), Korn (2010), and Naglik et al. (2015). Data for conch characteristics were obtained from longitudinal- and cross-sections for every 10 degrees (Fig. 1). Following Neige and Warnke (2010), we used the same anatomical landmark (dorsal attachment of the first septum) as the shell centre. Besides morphometry, CT-data are used for volumetric analyses, e.g., chamber volumes and surface areas.

For a consistent data description, the largest parameter, e.g., the diameter, is abbreviated with dm_1 while the parameter exactly 180 degrees (or half a whorl) earlier is abbreviated with dm_2. Basic conch parameters are the conch diameter (dm; dm_1, dm_2), whorl width (ww; ww_1, ww_2), whorl height (wh; wh_1, wh_2), whorl interspace (wi; wi_1, wi_2). All values of basic conch parameters are given in mm, surface areas in mm² and volumes in mm³.

We computed the following conch proportions and expansion rates (growth rates): Umbilical width (uw) $= dm1 - wh1 - wh2$; whorl expansion rate (WER) $= [dm1/(dm1 - wh1 - wi1)]2$; whorl width expansion rate (WWER) $= (ww1/ww2)2$; whorl height expansion rate (WHER) $= (wh1/wh2)2$; umbilical width index (UWI) $= uw1/dm1$; conch width index (CWI) $= ww1/dm1$; conch height index (CHI) $= wh1/dm1$ (= WHI of De Baets et al. 2013); whorl width index (WWI) $= ww1/wh1$; whorl interspace index (WII) $= wi1/wh1$.

Septal spacing, presented in angles, was quantified by using three different methods:

SDW = number of septa per 180 degrees or half a whorl and ASI_{20} = absolute septal index. The ASI_{20} refers to the number of septa counted along the ventral shell margin within a circle of 20 mm in diameter, which is perfectly aligned to the point where the whorl height is measured (Fig. 1). Similar to the quantifiers for rib spacing introduced by De Baets et al. (2013), the ASI is less influenced by coiling variability than SDW, and the SDW averages out possible short-term variation in septal spacing. The third approach uses angular measurements. Due to the extremely large angular values of the first few septa, plots begin with the fifth chamber (see supplement material for complete graphs). Chamber volumes and chamber surface areas are presented for each chamber as linear plots. For both parameters, we plotted the first 15 chambers in separate diagrams. Besides single chamber values, we graphed total volumes as well as the differences between succeeding chambers and differences in septal spacing for succeeding chambers. Furthermore, we compared surface area values against volumes in a Vogel number plot (see, e.g., Lemanis et al. 2016).

All 2D-measurements are presented as logarithmic plots, while septal spacing, chamber volumes and chamber surface areas are plotted against chamber number in a linear bivariate plot. Segmentation work was performed using Amira ZIB-Edition (Stalling et al. 2005). For the calculation of volumes based on CT-data, see Hoffmann et al. (2014) and Lemanis et al. (2015).

3 Results

Four *Spirula* shells (2015/0022/0001, 2015/0020/0007 and RUB-Pal 11250, 11255, Fig. 2-3) CT-scanned for this project will be described in the following paragraphs starting with 2D morphological data followed by volumetric data. Data from a fifth shell (RUB-Pal 11249) published by Hoffmann et al. (2015a) are used for the growth trajectory plots and in the discussion. Due to incomplete preservation of the shells BSPG 2014 XXI 88005-88007 and SNSB-BSPG 2018 I 21 and -22 (Figs. 4-9), however, the description is based on visual inspection of the shell and CT-data. Due to the lack of several juvenile chambers, the position of the morphological landmark could not be properly determined for these shells hampering a comparison with the other shells. The graphs for CHI, CWI, WHER, WWER, and ASI_{20} are included as supplementary material. We examined the live caught specimen only to obtain the volumes of the soft body and the mineralized parts (shell and statoliths) that we use in the discussion on the functional tolerance of the buoyancy apparatus.

Specimen 2015/0022/0001 - Maldives

The shell reaches 25.8 mm in diameter and has 37 chambers including the initial chamber (protoconch) with a total rotational angle of 853.5 degree, a total chamber volume of 919.5 mm³ (0.92 ml) and a total shell volume of 214.6 mm³. The largest chamber has a volume of 84.1 mm³. The surface of the shell from the Maldives shows a normal pattern, i.e. the shell surface is regularly crenulated. The shell dimensions increase or decrease more or less as expected, e. g., whorl height and whorl width and therefore also the whorl cross sectional area, decrease; WWI, WII, WER and Vogel number increase while SDW, septal spacing, chamber volume and surface area decrease near the end of ontogeny. (Fig. 2A, E, I, 9-11, Suppl. Fig. 3-4). A decreasing trend from six to four chambers during ontogeny was recorded for the ASI_{20} values (Supp. Fig. 4A). This is in accordance with a decreasing septal spacing during late ontogenetic stages but an increasing diameter (Fig. 11D). Volume differences vary between +10 (chamber 29) and -18 mm³ (chamber 35), which coincides with highest and lowest differences in surface areas (Fig. 11A). Towards the terminal aperture, the crenulated bands covering the shell surface become weaker, more inclined towards the aperture and finally vanish about 2-3 mm posterior of the final aperture, thus leaving the shell smooth except for straight-radial and parallel growth lines (Fig. 3A-B).

Specimen RUB-Pal 11250 - Fuerteventura

The shell reaches a diameter of 18.7 mm with 39 chambers (initial chamber only partially preserved) with a total rotational angle of 856.7 degrees, a total chamber volume of 503.8 mm³ and a total shell volume of 110.01 mm³. The largest chamber volume is 50.8 mm³. The surface of the shell is regularly crenulated except for the injured area that shows a smooth surface (Fig. 3D-E). The septum that formed directly after the injury is unusually thick and shows spherulitic carbonate crystals (Supp. Fig. 2D) comparable to specimen BSPG 2014 XXI 88006-7. Additionally, the injury affected the siphuncle and caused a slight dislocation (Fig. 3F, Supp. Fig. 2). The ontogenetic trajectories of the shell parameters show some distinct deviations from normal following the remarkable shell injury at 440-460 degrees (chamber 15) at a shell diameter of about 5 mm (Fig. 2F, 3D-E, 9; Supp. Fig. 3-4). The WER is the lowest among all examined specimens but was apparently only slightly affected, i.e. shows a more or less normal trend except for the injured area (Fig. 9C). The ontogenetic development of subsequent chamber volumes and chamber surface areas largely follow a normal trend but with the lowest values of all examined specimens.

Specimen 2015/0020/0007 – West Australia

The shell has a maximum diameter of 17.9 mm with 37 chambers excluding the missing initial chamber, a total chamber volume of 444.5 mm³, a total shell volume of 122.2 mm³, and a total rotational angle of 833.1 degrees. Ornamentation is not present on the earliest chambers and first occurs at a lateral position around the 8th chamber and slowly starts to cover the dorsal/ external area at about the 12th chamber. Chamber six (the fifth preserved chamber) is the most dramatically affected by the injury. This chamber forms a callus like thickening of the septum comparable to specimen RUB-Pal 11250 and BSPG 2014 XXI 88006-7 (Fig. 3G-I). The injury caused a larger fluctuation of WWI, WII, WER, SDW values (Fig. 9A-C, E), and the Vogel number (Fig. 11 C). Together with the shell RUB-Pal 11250, this specimen shares the lowest chamber volume and surface area values (Fig. 10-11).

In contrast to the ontogenetic perturbations, the specimen shows a clear terminal countdown morphology with increasing WER, WII and decreasing CHI, CWI, WHER, WWER, chamber volumes and chamber surface areas over the course of the last three preserved chambers.

Specimen RUB-Pal 11255 - Fuerteventura

The shell has a maximum diameter of 14.9 mm with 27 chambers preserved without the initial chamber, a total chamber volume of 296.9 mm³, a total shell volume of 77.85 mm³, and a total rotational angle of 682.1 degrees. Note that the original shell had eight more chambers with a total diameter of 20.4 mm and an additional half whorl (Supp. Fig. 1A). Unfortunately, the shell broke into two pieces prior to high-resolution scanning. The shell surface is regularly crenulated except for an area between the third- and fourth-last preserved septa. The fourth septum is associated with a significant swelling of the conch tube (= outer shell wall) followed by a smooth shell surface only at the right side of the shell. The median section reveals that the fourth septum is about 2-3 times thicker compared to the preceding and succeeding septa. A detailed inspection of the CT-data revealed that the septum broke off from the conch tube in a distinct area (Supp. Fig. 1D-G). The animal deposited several layers of the conch tube leading to the visible swelling. The specimen shows no abnormal pattern in the WWI, CHI, CWI, WHER, WWER, WII, SDW, or ASI_{20} including the terminal modifications (Supp. Fig. 1A, 3-4). All other shell parameter show only slight deviations compared to the Maldives shell (Fig. 9 C for WER, Suppl. Fig. 3-4). The increased septal thickness is expressed only in changes in septal spacing, chamber volume, surface area values, and the Vogel number (Fig. 10-11).

Specimen BSPG 2014 XXI 88005 – Gran Canaria

The shell has a maximum diameter of 17.5 mm with 21 preserved chambers. The earliest chambers, including the initial chamber, are not preserved. The shell has a preserved total rotational angle of about 450 degrees. The shell surface is regularly crenulated except for an area of about 90 degrees of the preserved most juvenile part of the shell (Fig. 4A, D). There, the shell shows a significant swelling associated with a blister pearl. The typical reticulate pattern disappears on one side and becomes significantly reduced on the opposite side of the shell in this particular area. The median section reveals that the blister occurs between chamber two and three but chamber four has a reduced septal spacing and chamber volume (Fig. 4C – star). The blister pearl is characterized by a small opening in both directions – inside towards the chamber and outside (Fig. 4D-K). A normal surface ornamentation pattern re-appears at the fifth chamber. The shell formed after the fifth chamber appears to follow a normal ontogenetic trend.

Specimen BSPG 2014 XXI 88006 – Gran Canaria

The scanned shell represents only a fragment of about 7 mm length, with four chambers, of a former intact shell with a total rotational angle of 810 degrees (see Keupp 2012, p. 346, fig. 435 top). The shell appears to follow the normal ontogenetic trend. The shell surface is regularly crenulated except for an area at about 40 degrees before the apertural end of the preserved shell. In that area, small shell fragments are covered with secondary shell layers (Fig. 5B). The very thin growth lines are somewhat irregular in that area. About 10 degrees beyond the last preserved aperture, the shell surface shows a discontinuity in shell growth (Fig. 5A). The median section reveals a significant thickening of the shell wall in this area (Fig. 5C, F). Shell thickening is accompanied by a decrease in septal spacing and irregularly shaped and unusually thick septa. In this area (Fig. 5E), the shell wall and septa become extremely thick. The last three septa are not fully mineralized, i.e. leaving an open connection between the chambers (Fig. 5F). Such a phenomenon was never reported before. Mineralization appears to be poor in parts, uncontrolled, and comprising spherulitic sectors. The siphuncle (Fig. 5C), however, is in its normal position.

Specimen BSPG 2014 XXI 88007 – Gran Canaria

The shell has a maximum diameter of 17.5 mm with 22 preserved chambers. The earliest chambers, including the initial chamber, are not preserved. All preserved chambers,

except for the last formed, appear normal. The shell has a preserved total rotational angle of about 470 degrees. The shell surface is regularly crenulated except for an area at about 30 degrees posterior of the apertural end of the preserved shell. Besides the normal pattern of vanishing crenulation on the shell surface, a thickening of the conch tube with spherulitic mineralization causes an irregular structure at the apertural margin, which also affects the septal surface (Fig. 6A-B, D-E). The median section (Fig. 6C, F close up) shows two distinct, thinly mineralized layers forming the penultimate septum. Some submicron thin calcareous layers were mineralized within the final chamber (Fig. 6F) and a few layers formed the surface of the final septum. The increased thickness of mineralized shell portions causes a dislocation of the siphuncle by about 45 degrees towards the centre of the chamber. No other irregularities are visible in earlier shell parts.

Specimen SNSB-BSPG 2018 I 21 – Gran Canaria

The shell has a maximum diameter of 16.2 mm with 29 preserved chambers. The initial chamber is not preserved. The shell shows a normal reticulate surface pattern until the 23rd chamber (Fig. 7). While the crenulation is present throughout ontogeny on one side, the opposite side shows an irregular pattern with smooth surface areas. The anomaly starts with a U-shaped structure followed by a slit-like band with backwards oriented growth lines that reach the apertural margin (Fig. 7B). The lateral and internal shell surface bear a rectangular shell fragment covered with secondary shell layers. Virtual sectional planes at that area reveal several healed shell fractures associated with a thickening of the conch tube (Fig. 7E-H). The septal spacing is reduced from chamber 23 to 24 and again between chambers 24 to 25, followed by an increase of septal spacing (Fig. 7D).

Specimen SNSB-BSPG 2018 I 22 – Gran Canaria

The shell has a maximum diameter of 12.7 mm with 14 chambers preserved. Large parts of the juvenile, and potentially adult, shell broke off (Fig. 8A-B). Similar to the shell BSPG 2014 XXI 88008, only one flank seems to be affected by this anomaly including the same phenomenon of areas with a smooth shell surface. The seven youngest preserved chambers exhibit a normal septal spacing when seen in median section. The eighth chamber, however, is significantly shorter - about one fifth of the preceding chamber. The associated eight septa share a similar thickness, while the ninth septum reaches three-times the normal thickness (Fig. 8D). A closer examination of the anomalous area revealed the presence of shell fragments (Fig. 8E) in the external part of the conch tube. Also the internal part and parts

of the siphuncle were affected (Fig. 8F). Surprisingly, a thorn-like shell fragment is found in the 8th chamber.

4 Interpretation

Specimen 2015/0022/0001 the "normal" shell

The ontogenetic development of the *Spirula spirula* shell from the Maldives is used as a morphological control, to compare with pathological shells. This enhances the distinction between different causes (external or internal) resulting in different morphological phenomena (syndromes). Morphological trends observed at the end of the preserved shell from the Maldives are: increasing WWI, WII, WER, SDW and Vogel number, and decreasing WHER, CHI, CWI, chamber volumes, chamber surfaces, and septal distances. All these morphological changes are summarized under the term "terminal countdown morphology" as introduced by Seilacher and Gunji (1993) and commonly seen in early ammonoids (e.g., De Baets et al. 2013, Stilkerich et al. 2017) to Cretaceous heteromorph ammonites (e.g., Delanoy et al. 1995, Ropolo 1995). Accordingly, we regard these changes as indicative for the adult stage of *Spirula spirula* (see also Hoffmann et al. 2015a). Besides ontogenetic changes in shell morphology, we also found changes in shell ornamentation. Namely, the final shell margin remains smooth except for straight, parallel growth lines. With increasing distance from the shell margin, a reticulate but strongly inclined shell ornamentation appears. First, growth lines become covered by a shell layer that is strongly inclined (not parallel to the growth lines). With increasing distances to the aperture a second shell layer form with an orientation more parallel, compared to the first layer, to the growth lines (Fig. 3B).

As far as we know, the only pathological shells of *Spirula spirula* were recently described by Keupp (2012) and show shell asymmetries, or displaced muscle attachment scars. The specimens with a "blister pearl" and additional shell material at the final shell margin described by Keupp (2012, Fig. 435, 436) have been re-examined for this study.

Specimen RUB-Pal 11250

This is the first report of a pathological *Spirula* shell with a likely exogenic origin, i.e. a predator attack, causing a sublethal injury (Keupp 2012; Hoffmann and Warnke 2014; Fig. 1B, F, J). Due to the internalization of the shell, sublethal injuries of the phragmocone occur more often compared to externally shelled cephalopods (nautiloids and ammonites) see Keupp (2012 for review). Based on the observations of the distribution of the reticulate surface

pattern, the affected siphuncle and the lower volume of chamber 15 (Fig. 2J), we assume that a predator attacked during the formation of this chamber. The predator broke the shell margin, which fell into the chamber and potentially damaged the rear soft body and mantle tissue. The broken part of the conch tube is covered by additional shell material and lies between the last normally formed septum and an unusually thick septum closing chamber 15. Besides its thickness, this septum also shows an irregular morphology. The inner surface of chamber 15 was not in contact with shell secreting tissue, neither during nor after the attack. In addition to the conch tube and septa, the siphuncle was affected. In the succeeding chamber, however, septal thickness and shape as well as the siphuncular tube exhibit a normal appearance, except for septal spacing. This suggests that the animal had partly or fully recovered from this traumatic event.

Specimen 2015/0020/0007

Although the external shell morphology differs significantly from the shell RUB-Pal 11250, the median section reveals some similarities. Namely, external shell material lies in the fifth preserved chamber and a significantly thicker sixth septum was developed (Fig. 3I arrow). While the earliest chambers appear to be pathological judging from their shell surface, the median section reveals that these are intact and of normal shape. Accordingly, we assume that a secondary layer of shell material that covers the original shell surface was deposited after the injury. The non-lethal injury most likely took place during the formation of the sixth (fifth preserved) chamber. At this point, mantle tissue was not in contact with the fifth preserved septum. Similar to the shell RUB-Pal 11250, shell formation quickly returns to normal shell thicknesses and shapes. Concerning, the conch tube growth, however, the animal was not able to follow the normal spiral course and precipitated an elliptical conch tube. This deviation might be related to an attack during early ontogeny or a more severe injury of distinct parts of mantle tissue that had not fully recovered.

Specimen RUB-Pal 11255

Potentially, the unusually thick septum broke off the shell wall (Supp. Fig. 1D-G). At that time, the septal mantle was still in contact with the septum and precipitated additional material to the septal surface and the inner surface of the conch tube to re-attach the septum to the conch wall. We suggest that the septum broke off the shell wall due to a predator attack. We assume that the injury caused by the supposed predator was less severe than those inflicted to specimens RUB-Pal 11250 and 2015/0020/0007. The reaction of the animal,

however, was similar to the other specimens in that a septum with increased thickness was precipitated and the succeeding chamber is smaller (reduced septal spacing and chamber volume; Fig. 2H, 3L).

Alternatively, the animal was pushed by a strong current against a solid object like a rock or boat; this appears rather unlikely, however, due to the deep-sea habitat of *Spirula* (Hoffmann and Warnke 2014). An associated parasite infection cannot be ruled out due to the blister-like morphology of the repaired conch wall (Supp. Fig. 1).

Specimen BSPG 2014 XXI 88005

Keupp (2012, p. 347) published this specimen previously, representing the first report of a brownish blister pearl in a shell of *Spirula spirula*. Blister pearl formation might have occurred by a disruption of the thin organic membrane between the two prismatic shell layers that built the conch wall. As a possible origin, Keupp (2012) discussed the presence of a parasite that settled at the actual shell margin between the mineralisation of inner and outer shell layers. Encapsulation of the modified tissue, including the parasite, may have caused the blister pearl formation and is comparable to other pearls of bivalves and ammonoids (Götting 1979; Keupp 1987; Ituarte et al. 2001, 2005; De Baets et al. 2011). An "in depth" review of this topic is provided by De Baets et al. (2015) and Huntley and De Baets (2015). A careful examination of the CT-data fully supports this hypothesis and indicates that parasites might affect shell formation in *Spirula*, visualized here with CT-data for the first time. It remains unclear, however, how the parasite entered the specimen and how long the parasite survived. Another hypothesis suggests an infection of the animal when the shell was covered by a very thin mantle tissue or was not covered with tissue at all (due to a rupture of the tissue). The two openings of the blister pearl suggest that the parasite lived as long as its host or the host was unable to seal the area completely.

Specimen BSPG 2014 XXI 88006

This specimen shows a pathology at its aperture (Fig. 5) comparable to that in BSPG 2014 XXI 88007. Due to a predator attack, shell fragments broke off the conch tube and injured the shell precipitating tissue (mantle). The small shell fragments were incorporated into the conch tube by secondary shell formation after the attack (Fig. 5B). The median section of the conch tube reveals that all four preserved septa are unusually thick and poorly mineralized (Fig. 5C). The siphuncular tube appears to be less affected, except for a shortening of the septal necks in adaptation to the shorter septal distances. Accordingly, it is

assumed that this specimen has survived the predator attack, although it suffered from the injury, but it could form a minimum of three chambers (maybe more). By injuring the mantle tissue, the attack disturbed shell mineralization and caused the loss of the ability to secrete new shell material in that particular area (Fig. 5D-E). Another median section shows that three of the four septa are not completely mineralized leaving an open area that connects the last three chambers with the inner soft body (Fig. 5F). As far as we know, this is the first report of an incompletely mineralized septum with an additional opening to the siphuncular tube. This may indicate that the specimen suffered from an inflammatory infection causing the poor mineralization of the septa with an opening (forma aegra *disseptata* Hölder 1956) serving to remove bacterial mucus. It should be noted here that this type of abnormality refers to a complete lack of septa. Partial mineralization of a septum or several septa, leaving a small non-mineralized part of the septum open, is unknown for any other cephalopod group. Taking this into account, the predator attack represented a second trauma possibly leading to the untimely death of the specimen.

Specimen BSPG 2014 XXI 88007

Except for the last two preserved chambers, the shell morphology exhibits a normal growth pattern (Fig. 6). Large amounts of secondary shell material were added externally and internally. The external shell surface shows the characteristic disappearance of ornamentation. This suggests that the injury occurred at the aperture when it was more or less positioned in the centre of the soft body. After the trauma, only a few millimetres of shell were added. Although it is hard to imagine such a syndrome as result of a predator attack, support for this interpretation comes from specimen BSPG 2014 XXI 88006 (see below; Fig. 6). The predator might have squeezed the whole body, causing a severe damage of its inner organs including the mantle tissue and here specifically the rear mantle sac. This attack disturbed the normal mineralization processes and the penultimate septum as well as the conch tube were formed by a number of poorly and irregularly mineralized layers. The presence of several layers forming one septum may indicate that it was temporarily impossible for the soft body to move forwards forming the next segment of conch tube. Temporary changes in septal spacing in relationship with trauma have also been observed in early ammonoids being infested by parasites. These affected both the aperture and septal spacing (e.g., De Baets et al. 2011, 2013b, 2015b, see also Keupp 2012, p. 240 for an overview). The last septum, instead, looks almost normal and thus suggests a more or less successful healing process with a reduced septal spacing. Probably, the next septum would

have developed in a normal distance with normal thickness and shape. Along the ventral shell wall, additional internal shell layers displace the siphuncle towards the middle of the conch tube. Dislocations of the siphuncle (forma aegra *juxtalobata* Hölder 1956) have been described for externally shelled ammonites by Hengsbach 1996 (see Review in Keupp 2012). Often the dislocation of the siphuncle, associated with an asymmetric septum, has been discussed as effects of parasitoses. In some ammonoid taxa, however, the position of the siphuncle seems to be more variable and, in some taxa, the asymmetric position of the siphuncle is species specific (e.g., *Anahoplites*, *Badouxia, Placenticeras*) suggesting that cephalopods have a high tolerance for displaced siphuncles (Longridge et al. 2009). A different pathogen that could have caused similar pathological phenomena is an inflammation of the mantle sac tissue – however we lack any supporting data for the latter interpretation. It is unclear whether the specimen reached adult-hood or not.

Specimen SNSB-BSPG 2018 I 21

The shell shows no signs of a trauma before the U-shaped structure on the shell surface appeared (Fig. 7B arrow). Since the abnormal pattern occurred only on one side of the shell creating a pattern similar to the forma aegra *verticata* (Hölder 1956), we assume that a predator attacked the animal and punctured the mantle tissue at the apertural margin (see Keupp 1992, 2012 and references therein). The longitudinal and cross sections of the shell reveals that not only was the tissue punctured but also material of the conch tube was fragmented (Fig. 7D-H, arrows indicate shell fragments). These fragments have been incorporated into the conch tube by the precipitation of secondary shell material after the traumatic event. After the predator attack, the animal successfully repaired its shell and returned to normal growth patterns and potentially reached adulthood.

Specimen SNSB-BSPG 2018 I 22

This shell exhibits a similar pathology as BSPG 2014 XXI 88008 (forma aegra *verticata*), which is restricted to one side. Again, no pathological phenomena are visible posterior of the injured area, which is characterized by the lack of surface crenulation (Fig. 8B, arrow). Median and cross sections of the shell revealed the presence of shell fragments partly pointing into the shell chamber (Fig. 8D-E). In addition, the siphuncular area is affected here (Fig. 8F, arrow). Similar to the specimens RUB-Pal 11250 from Fuerteventura and 2015/0020/0007 from West-Australia, the phragmocone is characterized by a significant

decrease of septal spacing between chambers seven and eight and a similarly large increase of septal spacing between chambers eight and nine. The preserved septa one to eight show similar thicknesses while septum nine appears two to three times thicker. Accordingly, we suggest that the predator attacked after formation of the eighth septum (mantle tissue is not in contact with the eighth septum), possibly during the formation of the ninth septum.

Specimen RUB-Pal 11249

The morphology of this shell has been described in detail by Hoffmann et al. (2015a). The shell shows no abnormal 2D shell morphology (Fig. 9). When it comes to volumetric and angular data, however, Hoffmann et al. (2015a) reported two significant deviations in septal spacing and associated chamber volumes during the course of ontogeny (see Fig. 10-11). Due to the development of a terminal countdown morphology, the specimen was fully grown. While speculating on the potential reasons that caused the fluctuations in septal spacing and chamber volume, Hoffmann et al. (2015a) excluded a pathogen as a trigger in favor of large environmental perturbations such as changes in water temperature, pH, salinity or simply the lack of food (Bucher et al. 1996; Kraft et al. 2008).

5 Discussion

While the interpretation largely focuses on the timing of pathologies and their cause and effect relation, the discussion focuses on the etiology of these pathologies.

5.1 Predator attack

Herein, we present the first CT-based evidence for phragmocone damage interpreted as the result of predator attacks on *Spirula* (specimens: RUB-Pal 11250 and 11255, 2015/0020/0007, BSPG 2014 XXI 88006-88007, SNSB-BSPG 2018 I 21 and -22). Sublethal, regenerated injuries are abundant phenomena in nautiloid and ammonoid shells but are restricted to the body chamber, except for a few cases (Kröger and Keupp 2004; Klug et al. 2008; Tsujino and Shigeta 2012; Keupp 2012, De Baets et al. 2013). Injuries in ectocochleate phragmocones are normally irreparable and cause an uncontrolled flooding of the affected chambers. In coleoids, with a chambered internal shell (aulacocerids, belemnites, sepiids, and spirulids), the mantle tissue completely encloses the shell (Naef 1922). Accordingly, injuries of the phragmocone are often sublethal and could be repaired (Keupp 2012). For example, Flower and McKenzie (1959) as well as Doguzhaeva et al. (2002) reported on carboniferous hematitids with sublethal, regular truncations of the initial phragmocone. For a non-

pathological interpretation of that phenomenon see Keupp (2012). Similarly, Mesozoic belemnites survived even more severe injuries leading to loss of parts of the rostrum and truncations of the phragmocone (Bandel and Kulicki 1988; Keupp 2002, 2012). Specifically, it has been reported that parts of the broken rostra remained within the shell sac and have been incorporated into the newly formed rostrum often resulting in a knee-like shape of the healed rostrum (Mietchen et al. 2005; Keupp 2012). We document a similar phenomenon here in several *Spirula* specimens incorporating shell fragments into the repaired conch tube (e.g., specimen BSPG 2014 XXI 88006; Fig. 5).

Injuries of exogenic origin are recognized as an indicator for possible predator-prey relationships. For the extinct ammonoids, palaeopathologies have been used to reconstruct preferred habitats, e.g., injuries from benthic crustaceans presumably indicate a nektobenthic or demersal life style (Keupp 2006, 2012; Ritterbush et al. 2014). Only a few reports about the predator and prey relationships are available for *Spirula*. Shells of *Spirula* were found as stomach contents of terns (Longley 1930), petrels and albatrosses (Imber 1973), tuna (Okutani and Suzuki 1975; Lansdell and Young 2007) and the cephalopod *Illex argentinus* (Santos and Haimovici 2002). *Spirula* mainly feeds on pelagic crustaceans such as copepods, ostracods among others, as evidenced by stomach contents (Kerr 1931; Nixon and Dilly 1977; Young 1977; Nixon and Young 2003). Observations of sterols support these findings but are also typical for other crustaceans like euphausids, small decapods and mysids that may also represent typical prey (Ballantine et al. 1981). Observed diel migration patterns of *Spirula* resemble the range of most pelagic crustaceans (Clarke 1969). Evidence for food sources other than decapods are not available. Recently, Ohkouchi et al. (2013) analysed nitrogen isotopes supporting the idea that *Spirula* predominantly fed on detritus and zooplankton.

It seems unlikely that a bird caused the shell damage because *Spirula*, under normal conditions, does not live near the sea surface. Birds only feed on *Spirula* when animals come to the sea surface due to problems with their buoyancy control or because of mortality after spawning. Planktonic crustaceans, prey items of *Spirula*, are too small to cause such large injuries, and benthic crustaceans can be excluded because *Spirula* lives in the open water column. The remaining potential predators are fish and other coleoids. The pathologies observed in specimens SNSB-BSPG 2018 I 21 and -22 resemble forma aegra *verticata* and could have been caused by coleoids or crustaceans (Keupp 2012).

5.2 Parasitism

Herein, we present the first CT-based indication for a parasitic infection of a *Spirula* shell (BSPG 2014 XXI 88005). As far as the authors know, there is only one additional report on a parasite for *Spirula* by Jepps (1931, in Kerr 1931 as appendix, p. 35-36). Therein, Jepps (1931) and Kerr (1931) reported on large numbers of parasites in the renal spaces and one in the coelomic spaces around the pancreas. The parasites have been identified as ciliates (Ciliophora: *Chromidina elegans* following Pascual et al. 1996). Interestingly, the same species have been reported from *Sepia elegans*, *S. orbignyana*, *Loligo* sp., *Illex coindetii*, *Todarodes sagittatus*, *Octopus salutii*, and *Loligo* sp. (Jepps 1931, Souidenne et al. 2016). This may indicate that these species make use of the same food resources, possess overlapping habitat ranges or feed on each other. Otherwise, it could also mean that the parasite as a relatively wide distribution in terms of water depth and host specimens (Priede 2017, Bray 2004) Parasite richness in cephalopods is highly variable at the species and genus level (Hochberg 1990). These differences in parasite richness were used to reconstruct the ecological conditions of the biotopes, i.e., the vertical and horizontal structure of ecosystems that different cephalopod species inhabit.

Most studies about modern molluscan parasites deal with parasites of bivalves. Bivalve molluscs are hosts of a diverse group of parasites and disease-causing agents, e.g., viruses, prokaryotes, fungi, protists, parazoans, and metazoans (platyhelminths, annelids, molluscs, bryozoans, and arthropods; see Lauckner 1983 and Huntley and De Baets 2015 for extensive reviews). Most of the parasites belong to endoparasitic flukes (Trematoda, Digenea), which can also be found in gastropods, a closely related mollusc group (Ozanne and Harries 2002; Littlewood and Donovan 2003; Huntley and De Baets 2015). Larvae of digenean trematodes (Gymnophallidae) sometimes lead to the formation of pearls (Ituarte et al. 2001; Cremonte and Ituarte 2003; Littlewood and Donovan 2003; Huntley and De Baets 2015) and have also been found in fossil bivalves dating back to the Triassic (Boucot and Poinar 2011) and possibly even the Palaeozoic (Klug et al. 2008; De Baets et al. 2011). Pearl formation, however, can have a variety of causes, many of which are not due to parasites (Lauckner 1983). For example, De Baets et al. (2011) reported pearls in ammonoid shells that do not match with the patterns modern digeneans leave in bivalve shells (Lauckner 1983; Cremonte 2004; Leung 2017, see also De Baets et al. 2015; Huntley and De Baets 2015).

Like in other reports on parasitism in cephalopods, all parasites infested different parts of their soft tissues, e.g. the gills, mantle cavity or digestive tract (McLean et al. 1987; Hochberg 1990; Hanlon and Forsythe 1990; Pascual et al. 1996, 2007; Gestal et al. 1999;

Gonzalez et al. 2003; Castellanos-Martínez and Gestal 2013) but none were reported to infest the mineralized shell. For *Nautilus* only copepods have been described that do not enter between the shell and mantle (De Baets et al. 2015b), and from a *Nautilus* in captivity, a helminth (Nematoda) has been reported by Barord et al. (2012) – neither can explain the observed pattern. Given that cephalopods are a key trophic element in modern and ancient marine communities (Clarke 1996), it is no surprise that Hochberg (1990) documented 200 endoparasitic species in cephalopods with macroparasites, e.g., nematodes, copepods, and isopods.

Recently, Keupp (2012) described a *Spirula* shell with a blister pearl speculating on a parasitic infection during shell formation and compared it with similar blister pearl-like structures on the inner surface of bivalves and ammonites (Götting 1979; Keupp 1987). Although difficult to detect, because parasites are often very small and soft bodied, it is even more complicated to identify the parasite after its soft body has decomposed (Conway Morris 1981; De Baets et al. 2015b; Leung 2017). This largely depends on the fact that different parasites can lead to similar reactions of the host due to convergence in the evolution of host exploitation strategies (Littlewood and Donovan 2003; De Baets et al. 2015b; Leung 2017). Following the outlines given by Götting (1979), Ituarte et al. (2001, 2005) as well as in the review by Huntley and De Baets (2015), the igloo-shaped blister pearl with its opening is most likely induced by a digenean trematode parasite. While igloo-shaped blister pearls have only one opening, the presence of two openings have often been attributed to phoronids (Bassett et al. 2004; Vinn et al. 2014).

5.3 Inflammation

Here, we present the first CT-based evidence for inflammation of *Spirula spirula* (BSPG 2014 XXI 88006). The main argument put forward is that the mechanical fragmentation of the shell due to an assumed predation attempt was limited to the apertural margin and accordingly could not explain the four pathological septa. Taking this into account, an endogenic reason like a parasitosis or bacterial infection appears likely to explain that particular progressive phenomenon. Keupp (2012) described a pathological belemnite rostrum with an open-drainage channel, which probably had formed as the result of an inflammation of the shell precipitating tissue. This interpretation, however, remains highly speculative until further evidence is found. The perforation of the septa could also indicate the presence of an endoparasite that moved together with the rear body during the chamber formation process.

5.4 Effects of pathologies on the shell shape

While the discussion above incorporates all examined shells, the discussion about the effect on shell shape changes and on the efficiency of the buoyancy apparatus is limited to the following five specimens: 2015/0022/0001, 2015/0020/0007 and RUB-Pal 11249-11250, and 11255 (Fig. 2-3).

As pointed out by De Baets et al. (2015a), individuals of cephalopods that belong to the same species vary morphologically, i.e. in size, and shape. *Spirula spirula* with its internal shell superficially resembles, but does not belong to, heteromorph ammonites with an external shell. For those shells, a number of characteristic features (see method part) are used to describe their shell morphology. Quantification of these shell parameters is of great importance in order to recognize intraspecific variability. Neglecting intraspecific variability can lead to taxonomic oversplitting or lumping, i.e., modulated taxonomy and taxonomic richness (palaeodiversity; see De Baets et al. 2013, 2015a). In the case of *Spirula*, the actual number of extant species was questioned (Warnke 2007; Neige and Warnke 2010). The reason for this was the scattered geographic distribution of seemingly isolated *Spirula spirula* populations around the globe and the lack of an adequate morphological description of the type material (Hoffmann and Warnke 2014; Nikolaeva 2015; Lukeneder 2016). The morphological variation of the different populations (ecophenotypes) of specimens of a single species may lead to an erroneous assignment to different morphospecies. In order to solve this, Neige and Warnke (2010) as well as Lukeneder (2016) employed quantitative measurements, e. g., whorl height against radius or diameter and septal spacing/ radius, whorl width against diameter, whorl height/ whorl width against diameter, of different shell parameters and ratios without a robust conclusion on the number of valid species.

Here, we explore the extreme limits of morphological variability by quantifying the morphology of pathological shells. These extreme morphological end-members provide an idea of the potential extent of intraspecific variability for *Spirula spirula*.

The WWI significantly differs between the Maldives specimen 2015/0022/0001 and specimen 2015/0020/0007 (W-Australia) starting with a significant drop to 0.6 where the injury occurs and remains consistently lower during ontogeny but with an increasing trend (up to 1.1 at the end of the shell). The specimen RUB-Pal 11250 shows significantly higher values around the injured diameter (around 1.3 compared to 1.1 for the shell form the Maldives) with a rapid decreasing trend back to normal values. Due to the elliptic shell shape, the WII strongly deviates (becoming 0.0) from the normal (ranging between 0.1 and 0.2). The other

shells show no significant deviation in their values. The WER is significantly and continuously lower in the specimens 2015/0020/0007 and RUB-Pal 11250. Large sinuous fluctuation of UWI values occur in the same specimens 2015/0020/0007 and RUB-Pal 11250. RUB-Pal 11249 appears to have slightly but continuously higher values. The specimen with the single thick septum (RUB-Pal 11255) shows no significant deviations from normal values for WWI, WII, WER, UWI, and SDW. Although more or less heavily injured (RUB-Pal 11249 not injured), all specimens show the terminal countdown morphology with an increase in WWI, WII, WER, and Vogel number, as well as decreasing WHER, CHI, CWI, septal spacing, chamber volumes and inner chamber surface areas.

5.5 Functional tolerance of the buoyancy apparatus

All modern cephalopods with a chambered shell acting as buoyancy device achieve approximately neutral buoyancy by changing the gas/ liquid ratio in their shell chambers via the siphuncle (Denton 1971, 1974; Hoffmann et al. 2015b). Addition or loss of shell material observed in the pathological shells of *Spirula* has to be compensated by the animal to maintain neutral buoyancy. A reduction of the body chamber length as discussed for ammonoids is not possible due to the internal position of the shell and the largely reduced body chamber in *Spirula*. However, a decrease in soft tissue growth could compensate for additional shell material. Another option to compensate for changes in shell weight is the reduction or addition of cameral liquid. Retained liquid can serve as ballast water for buoyancy regulation (Denton 1974). Interestingly, Denton et al. (1967) described the presence of cameral liquid not only within the latest formed chambers but also within the earliest (juvenile) chambers. Finally, a third option could be a reduced thickness of the subsequent shell wall and septa at the risk of a mechanically weaker shell or changes in the shell volume / chamber volume ratio, suggesting relatively larger chambers.

There are many unknown factors, such as soft body volume and density or the amount of liquid kept in the chambers (see Hoffmann et al. 2015b, Lemanis et al. 2015 for details). Therefore, a necessarily rough approach to the buoyancy calculations for the examined *Spirula* shells is used here to gather first insights on the impact of the pathologies on the buoyancy apparatus of *Spirula*. In order to do this, two versions of each of the three pathological shells used here were created. One version contained the shell modified by the pathology and the other version had a non-pathological shell; all other parameters were kept constant between these two versions. Neutral buoyancy is achieved when the weight of the animal is equal to the weight of the fluid volume displaced by the animal. We presume that all

chambers are dry and contain no liquid and that the gas does not contribute to the animal's weight and the mantle cavity is filled with water. For the mineral density, a mean value of 2.6 g/cm³ and for the soft body 1.05 g/cm³ is used, while for seawater, a mean density of 1.026 g/cm³ is used (see Hoffmann et al. 2015b, Lemanis et al. 2015 for details). The effects of the change in shell volume would be greatest at the time the pathology occurred. All of the pathological shells were manually re-segmented in order to remove the shell after the pathology such that the pathological chamber would be the last formed chamber. The non-pathological shell from the Maldives was altered to the same number of chambers in order to compare a pathological shell to a healthy shell of the same size. In order to get volume estimates for parts of the body, ratios between the shell volume and other volumes are made based on CT data of a complete *Spirula* animal (Fig. 12). We calculated the ratios: statolith volume to shell volume (= 0.007), mantle cavity volume to shell volume (= 12.4), and soft body volume to shell volume (= 52.1). Values for the volume of the statoliths, mantle cavity, and soft body were the same in the pathological and non-pathological shells so that the only variation occurred in the shell and chamber volume. The documented slight differences in size are regarded here as negligible.

➔ About here Table2

Comparisons between calculated buoyancy values show relatively small differences between the pathologic and non-pathologic shells (Table 2). Of the three shells, two are negatively buoyant and one is positively buoyant. It is important to note that the relative sizes of parts of the animal change through ontogeny. Nevertheless, a lack of volumetric data prevents us from considering this in these calculations. The specimen used to create the ratios possessed 26 chambers while the RUB-Pal 11250 has 16 chambers, 2015/0020/0007 has 7 chambers, and RUB-Pal 11255 has 25 chambers.

The positive buoyancy of RUB-Pal 11255 permits a theoretical calculation of the amount of fluid, here 69.7 mm^3 or 32.6% of the total chamber volume, which would have to be present in the chambers to achieve neutral buoyancy. For an equivalent, non-pathological shell, 55.6 mm^3 of fluid representing 31.2% of the total chamber volume would have to be present. Like the buoyancy calculations, this comparison shows that the pathology has a relatively minor contribution to the animal's buoyancy. This is not very surprising considered that the contribution of the shell to the total volume (about 8%) and weight (about 0.2 g) of the animal is small relative to the soft tissue. It seems likely that such small differences in

buoyancy have been compensated by the animal by a) jet propulsion, b) fin movement, and c) a slow refill of the chambers with liquid (Ward 1982 for the siphuncular index of *Spirula*).

6 Conclusion

We present the first application of high-resolution CT-data to study pathological *Spirula spirula* shells. The pathological shells have been compared with a non-pathological shell as normal-standard to evaluate deviations in shell morphology. Our study is, however, limited to the comparison of pathological shells with one normal shell (not a normal population) leaving out the discussion about intraspecific variability of shell morphology. Although analyses of CT-data reveal several shells having severe injuries due to predator attacks, one shell was infested by a parasite, potentially a digenean trematode, causing the formation of a blister-pearl, and another shell shows signs of an inflammation. Lacking direct evidence, coleoids or fishes have been discussed as potential predators. Fluctuation of chamber volumes without signs of injuries are preliminary regarded as indicator for stressed environments. To assess the functional tolerance of the buoyancy apparatus, three pathological shells were compared with soft tissue volume and shell volume ratio of an actual specimen. Results suggest that all examined pathologies had minor impact on buoyancy.

Acknowledgements:

The authors are grateful to A. Nützel for lending us two pathological *Spirula* shells for our study. Kerstin Warnke provided us with a live caught specimen of *Spirula* that is used for the evaluation of the functional tolerance of the buoyancy apparatus. RH acknowledges the DFG for financial support DFG HO-4674/4-1. The authors greatly appreciate the constructive reviews provided by K. De Baets and two anonymous reviewers. Further, we are grateful to the Editor in Chief (I. Priede) and the Associated Editor (H.J.T. Hoving) for considering our contribution for publication.

Compliance with Ethical Standards

Funding:
This study was funded by DFG (grant Ho4674/4-1).

Conflict of Interest:
I, René Hoffmann, hereby declare that on behalf of all co-authors, we have no conflict of interest.

Ethical approval :
All applicable international, national, and/or institutional guidelines for the care and use of animals were followed.

Significance

Here we report for the first time on high resolution computed-tomography data of pathological shells of the enigmatic deep sea coleoid *Spirula spirula*. Pathological phenomena (syndroms) of mineralized hardparts (e.g., bones or shells) represent a unique source of information that can help to better understand the ecology or life modes of organisms that are either difficult to observe in their natural habitat or extinct. Studies of pathological specimens are largely restricted to surface evaluations due to reluctance to damage such rare materials. The internal shell of *Spirula spirula* is of particular interest because of the loosely coiled shell resembling the shell morphologies of Early Devonian and some Cretaceous (heteromorphs) extinct ammonoids. We quantify the shell morphology of these pathological shells, representing deviations from the "normal" phenotype, to explore the potential limits of shell morphospace. Knowledge about the range of shell variation can help to disentangle the question how many valid species exist in the genus *Spirula*. Furthermore, we explore the cause and effect of pathologies in *Spirula* that are often related to predator attack by fishes or coleoids, one inflammation, and in one case by an endogenic parasite. These trauma induced changes of the shell morphology also add additional weight due to the production of additional shell material. Changes of shell volume / chamber volume ratios were assessed to evaluate the functional tolerance of the buoyancy apparatus. Fluctuation of chamber volumes without signs of injuries are regarded as an indicator for stressed environments.

References

Appellöf A (1893) Die Schalen von *Sepia*, *Spirula* und *Nautilus* - Studien über den Bau und das Wachstum. Kongl. Svenska Vetenskaps-akademiens Handlingar 25: 1-106.

Ballantine JA, Roberts JC, Morris RJ (1981) Sterols of the cephalopod *Spirula spirula.* J. mar. Biol. Ass. U.K. 61: 843-850.

Bandel K, Kulicki C (1988) *Belemnoteuthis polonica*: A belemnite with an aragonitic rostrum. In: Wiedmann J, Kullmann J (eds) Cephalopods Present and Past, Schweizerbart, Stuttgart, pp 247-271.

Barord GJ, Ju C, Basil JA (2012) First report of a successful treatment of a mucodegenerative disease in the chambered nautilus (*Nautilus pompilius*). Journal of Zoo and Wildlife Medicine 43: 636-639.

Bassett, MG, Popov LE, Holmer LE (2004) The oldest-known metazoan parasite?. Journal of Paleontology 78: 1214-1216.

Bello G, Paparella P (2003) Scar bearing cuttlebones in wild-collected *Sepia orbignyana* (Cephalopoda: Sepiidae) and the effects of scar occurrence on morphometrics relationships. Berliner Paläobiologische Abhandlungen 3: 13-18.

Boucot AJ, Poinar Jr GO (2011) Fossil Behavior compendium. CRC Press, Boca Raton, FL.

Boletzky Sv, Overath H (1989) Shell fracture and repair in the cuttlefish *Sepia officinalis*. In: Boucaud-Camou È (ed) La Seiche, The cuttlefish, 1. International Symposium on the Cuttlefish *Sepia*, Caen, pp 69-78.

Bray RA (2004) The bathymetric distribution of the digenean parasites of deep-sea fishes. Folia Parasitologica 51: 268-274.

Bruun AF (1943) The Biology of *Spirula spirula*. The Carlsberg Foundation´s Oceanographical Expedition Round the World 1928-30 and Previous "Dana"-Expeditions; Dana Report 24: 1-44.

Bruun AF (1955) New light on the Biology of *Spirula*, a mesopelagic Cephalopod. Essays in the Natural Sciences in honour of Captain Allan Hancock on the occasion of his birthday, July 26, 1955 12: 61-71.

Bucher H, Landman NH, Klofak SM, Guex J (1996) Mode and rate of growth in ammonoids. In: Landman NH, Tanabe K, Davis RA (eds) Ammonoid paleobiology, Topics in Geobiology 13, Springer, pp 359-426

Castellanos-Martínez S, Gestal C (2013) Pathogens and immune response of cephalopods. Journal of Experimental Marine Biology and Ecology 447: 14-22.

Chun C (1910) *Spirula australis*. Berichte der Mathematischen-Physischen Klasse der Königlich Sächsischen Gesellschaft der Wissenschaften zu Leipzig 62: 173-188.

Chun C (1915) The Cephalopoda Part 1: Oegopsida, Part 2: Myopsida, Octopoda - Text and Atlas. Scientific Results of the German Deepsea Expedition on Board the Steamship "Valdivia" 1898-1899 ,18.

Clarke MR (1969) Cephalopoda collected on the SOND cruise. Journal of Marine Biological Assoziation U.K. 49: 961-976.

Clarke MR (1970) Growth and development of *Spirula spirula*. Journal of Marine Biological association U.K. 50: 53-64.

Clarke MR (1978) The cephalopod Statolith – an introduction to its form. Journal of the Marine Biological Association U.K. 58: 701-712.

Clarke MR (1996) The role of Cephalopods in the World's oceans: General conclusion and the future. Philosophical Transactions, Biological Sciences 351: 1105-1112.

Conway Morris S (1981) Parasites and the fossil record. Parasitology 82: 489-509.

Cremonte F (2004) Life cycle and geographic distribution of the gymnophallid *Bartolius pierrei* (Digenea) on the Patagonian coast, Argentina. Journal of Natural History 38: 1591-1604.

Cremonte F, Ituarte C (2003) Pathologies elicited by the gymnophallid metacercarie of *Bartolius pierrei* in the clam *Darina solenoides*. J. Mar. Biol. Asso. U.K. 83: 311-318.

Dauphin, Y (1976): Microstructure des coquilles de Cephalopodes. 1. *Spirula spirula* L. (Dibranchiata, Decapoda). Bulletin du Muséum National D´Histoire Naturelle, troisième série 382: 197-238.

De Baets K, Klug C, Korn D (2009) Anetoceratinae (Ammonoidea, Early Devonian) from the Eifel and Harz Mountains (Germany), with a revision of their genera. Neues Jahrbuch für Geologie und Paläontologie Abhandlungen 252: 361-376.

De Baets K, Klug C, Korn D (2011) Devonian pearls and ammonoids-endparasite co-evolution. Acta Palaeontologica Polonica 56: 159-180.

De Baets K, Klug C, Monnet C (2013) Intraspecific variability through ontogeny in early ammonoids. Paleobiology 39: 75-94.

De Baets K, Klug C, Korn D, Bartels C, Poschmann M (2013b) Emsian Ammonoidea and the age of the Hunsrück Slate (Rhenish Mountains, Western Germany). Palaeontographica A 299: 1-113.

De Baets K, Bert D, Hoffmann R, Monnet C, Yacobucci MM, Klug C (2015a) Chapter 9 – Ammonoid intraspecific variability. In: Klug C, Korn D, De Baets K, Kruta I, Mapes RH (eds) Ammonoid paleobiology: From anatomy to ecology, Springer, pp 359-426.

De Baets K, Keupp H, Klug C (2015b) Parasites of ammonoids. In: Klug C, Korn D, De Baets K, Kruta I, Mapes RH (eds) Ammonoid paleobiology: From anatomy to ecology, Springer, pp 837-875.

Delanoy G, Ropolo P, Magnin A, Autran G, Poupon A, Gonnet R (1995) On the dimorphism in the Ancyloceratina (Ammonoidea) from Lower Cretaceous. Comptes Rendus de l´Academie des Sciences Serie II Fascicule A-Sciences de la Terre et des planetes 321: 537-543.

Denton EJ (1971) Examples of the use of active transport of salts and water to give buoyancy in the sea. Phil. Trans. R. Soc. London B 262: 277-287.

Denton EJ, Gilpin-Brown JB (1971) Further observations on the buoyancy of *Spirula*. Journal of the Marine Biological Association U.K. 51: 363-373.

Denton EJ (1974) On buoyancy and the lives of modern and fossil cephalopods. Proc. R. soc. London B 185: 273-299.

Denton EJ, Gilpin-Brown JB, Howarth JV (1967) On the buoyancy of *Spirula spirula*. Journal of the Marine Biological Association U.K. 47: 181-191.

Doguzhaeva LA, Mapes RH, Mutvei H (2002) Early Carboniferous coleoid *Hematites* Flower and Gordon, 1959 (Haematitida ord. nov.) from Midcontinent (USA). Abhandlungen der geologischen Bundesanstalt Wien 57: 299-320.

Flower RH, Mackenzie G (1959) More Mississippian Belemnites. Journal of Paleontology 33: 809-842.

Gestal C, Belcari P, Abollo E, Pascual S (1999) Parasites of cephalopods in the northern Tyrrhenian Sea (western Mediterranean): new host records and host specificity. Scientia Marina 63: 39-43.

Giovannetti G, Guerrini A, Salvadori PA (2016) Magnetic resonance spectroscopy and imaging for the study of fossils. Magnetic Resonance Imaging 34: 730-742.

Götting KJ (1979) Durch Parasiten induzierte Perlbildung bei *Mytilus edulis* L. (Bivalvia). Malacologia 18: 563-567.

González AF, Pascual S, Gestal C, Abollo E, Guerra A (2003) What makes a cephalopod a suitable host for parasite? The case of Galician waters. Fisheries Research 60: 177-183.

Gonzalez R, Gallina PA, Cerda IA (2017) Multiple paleopathologies in the dinosaur Bonitasaura salgadoi (Sauropoda: Titanosauria) from the Upper Cretaceous of Patagonia, Argentina. Cretaceous Research 79: 159-170.

Grauer AL (2012) A Companion to Palaeopathology. Blackwell, New Jersey.

Guex J (1967) Contribution à l´étude des blessures chez les ammonites. Bulletin des Laboratoires de Géologie, Minéralogie, Géophysique et du Musée Géologique de l´Université de Lausanne 165: 1-16.

Halstead LB (1990) 4.15 Palaeopathology - In: Palaeobiology A Synthesis, pp 381-385.

Hanlon RT, Forsythe JW (1990) Diseases of Mollusca: Cephalopoda. In: Kinne O (ed) Diseases of Marine Animals Vol. III. Cephalopoda to Urochordata, Biologische Anstalt Helgoland, Hamburg, pp 203-205.

Hengsbach R (1996) Ammonoid pathology. In: Landman NH, Tanabe K, Davis RA (eds) Ammonoid paleobiology. Topics in Geobiology 13: 581-605.

Hochberg FG (1990) Diseases of Mollusca: Cephalopoda. In: Kinne O (ed) Diseases of marine animals Vol. III. Cephalopoda to Urochordata. Biologische Anstalt Helgoland, Hamburg, pp 47-227 pp.

Hoffmann R, Warnke K (2014) *Spirula* - das unbekannte Wesen aus der Tiefsee (*Spirula* - the unknown deep sea creature). Denisia 32: 33-46.

Hoffmann R, Schultz JA, Schellhorn R, Rybacki E, Keupp H, Gerden SR, Lemanis R, Zachow S (2014) Non-invasive imaging methods applied to neo- and paleontological cephalopod research. Biogeosciences 11: 2721-2739.

Hoffmann R, Keupp H (2015) Ammonoid Paleopathology. In: Klug C, Korn D, De Baets K, Kruta I, Mapes RH (eds) Ammonoid paleobiology: From anatomy to ecology, Springer, pp 877-926.

Hoffmann R, Reinhoff D, Lemanis R (2015a) Non-invasive imaging techniques combined with morphometry: a case study from *Spirula*. In: Klug C, Hoffmann R, Fuchs D, Marty D (eds) Special Issue – Recent advances in Cambrian to modern cephalopod research I. Swiss Journal of Palaeontology 134, pp 207-216.

Hoffmann R, Lemanis R, Naglik C, Klug C (2015b) Ammonoid buoyancy. In: Klug C, Korn D, De Baets K, Kruta I, Mapes RH (eds) Ammonoid paleobiology: From anatomy to ecology, Springer, pp 613-648.

Hoffmann R, Ansorge J, Wesendonk H, Stevens K (2018) A Late Cretaceous pathological belemnite rostrum with evidence of infection by an endoparasite. Neues Jahrbuch für Geologie und Paläontologie Abhandlungen 287: 335-349.

Hölder H (1956) Über Anomalien an jurassischen Ammoniten. Paläontologische Zeitschrift 30: 95-107.

Huntley JW, De Baets K (2015) Trace fossil evidence of trematode-bivalve parasite-host interactions in deep time. Advances in Parasitology 90: 201-231.

Huxley, HT, Pelseneer P (1895) Observations sur *Spirula*. Bulletin Scientifique de la france et de la Belgique 1895: 1-47.

Imber MJ (1973) The food of Grey-faced Petrels (*Pterodroma macroptera gouldi* (Hutton)), with special reference to diurnal vertical migration of their prey. Journal of Animal Ecology 42: 645-662.

Imperadore P, Fiorito G (2018) Cephalopod Tissue Regeneration: Consolidating over a century of knowledge. Frontiers in Physiology 9:593: 1-21.

Ituarte CF, Cremonte F, Deferrari G (2001) Mantle-shell complex reactions elicited by digenean metacercarie in *Gaimardia trapesina* (Bivalvia: Gaimardiidae) from

the south-western Atlantic Ocean and Magellan Strait. Diseases of Aquatic Organisms 48: 47-56.

Ituarte C, Cremonte F, Zelaya DG (2005) Parasite-mediated shell alterations in Recent and Holocene sub-Antarctic bivalves: the parasite as modeler of host reaction. Invertebrate Biology 124: 220-229.

Jepps MW (1931) Appendix: On a parasitic ciliate from *Spirula*. Dana Expeditions 8: 35-36.

Kabanov GK (1967) Skelet belemnitid. Morfologiya i biologicheskii analiz. Trudy Paleontologicheskogo Instituta, Akademii Nauk SSSR 114: 1-117.

Kerr JG (1931) Notes upon the Dana specimens of *Spirula* and upon certain problems of cephalopod morphology. The Danish "Dana"-Expeditions 1920-22 in the North Atlantic and the Gulf of Panama, Dana Expedition 8: 1-36.

Keupp H (1973) Der Wert anomaler Perisphincten (Ammonoidea) für die Deutung der Parabelgenese. Geologische Blätter NO-Bayern 23: 20-35.

Keupp H (1984) Pathologische Ammoniten: Kuriositäten oder paläobiologische Dokumente? Teil 1. Fossilien 1984/6: 258-262.

Keupp H (1985) Pathologische Ammoniten: Kuriositäten oder paläobiologische Dokumente? Teil 2. Fossilien 1985/1: 23-35.

Keupp H (1987) Perlen (Schalenkonkretionen) bei Dactylioceraten aus dem fränkischen Lias. Jahresmitteilungen der Naturhistorischen Gesellschaft Nürnberg 1986: 97-102.

Keupp H (1992) Rippenscheitel bei Ammoniten-Gehäusen. Fossilien 1992/5: 283-290.

Keupp H (2000) Ammoniten – Paläobiologische Erfolgsspiralen. Thorbecke, Stuttgart

Keupp H (2002) Pathologische Belemniten: Schein und Wirklichkeit. Fossilien 2002/2: 85-92.

Keupp H (2006) Sublethal punctures in body chambers of Mesozoic ammonites (forma aegra *fenestra* n.f.), a tool to interpret synecological relationships, particularly predator-prey interactions. Paläontologische Zeitschrift 80: 112-123.

Keupp H (2012): Atlas zur Paläopathologie der Cephalopoden. Berliner Paläobiologische Abhandlungen 10: 1-390.

Keupp H, Fuchs D (2014): Different regeneration mechanisms in the rostra of aulacocerids (Coleoidea) and their phylogenetic implications. Göttingen Contributions to Geosciences 77: 13-20.

Keupp H, Mitta V (2004) Septenbildung bei *Quenstedtoceras* (Ammonoidea) von Saratov (Russland) unter anomalen Kammerdruckbedingungen. Mitteilungen des Geol.-Paläont. Instituts der Universität Hamburg 88: 51-62.

Klug C (2007) Sublethal injuries in Early Devonian cephalopod shells from Morocco. Acta Palaeontologica Polonica 52: 749-759.

Klug C, Hoffmann R (2015) Chapter 3 - Ammonoid Septa and Sutures - In: Klug C, Korn D, De Baets K, Kruta I, Mapes RH (eds) Ammonoid Paleobiology: From Anatomy to Ecology, Springer, pp 45-90.

Klug C, Kröger B, Rücklin M, Korn D, Schemm-Gregory M, De Baets K, Mapes RH (2008) Ecological change during the early Emsian (Devonian) in the Tafilalt (Morocco), the origin of the Ammonoidea, and the first African pyrgocystid edrioasteroids, machaerids and phyllocarids. Palaeontographica A 283 (1, 2): 1-94.

Klug C, Meyer EP, Richter U, Korn D (2008) Soft-tissue imprints in fossil and Recent cephalopod septa and septum formation. Lethaia 41: 477-492.

Korn D (2010) A key for the description of Palaeozoic ammonoids. Fossil Record 13: 5-12.

Korn D, Klug C (2007) Conch form analysis, variabilitiy, morphological disparity, and mode of life of the Frasnian (Late Devonian) ammonoid *Manticoceras* from Coumiac (Montagne Noire, France). In: Landman NH, Davis RA, Mapes RH (eds) Cephalopods Present and Past New Insights and Fresh Perspectives, Springer, pp 57-85.

Kraft S, Korn D, Klug C (2008) Patterns of ontogenetic septal spacing in Carboniferous ammonoids. Neues Jahrbuch für Geologie und Paläontologie Abhandlungen 250: 31-44.

Kröger B (2000) Schalenverletzungen an jurassischen Ammoniten - ihre paläobiologische und palökologische Aussagefähigkeit. Berliner Geowissenschaftliche Abhandlungen E 33: 1-97.

Kröger B, Keupp H (2004) A paradox survival - report of a repaired *syn vivo* perforation in a nautiloid phragmocone. Lethaia 37: 439-444.

Kröger B, Vinther J, Fuchs D (2011) Cephalopod origin and evolution: A congruent picture emerging from fossils, development and molecules. Bioessays 33: 602-613.

Lansdell M, Young J (2007) Pelagic cephalopods from eastern Australia: species composition, horizontal and vertical distribution determined from the diets of pelagic fishes. Rev. Fish. Biol. Fisheries 17: 125-138.

Lauckner G (1983) Diseases of Mollusca: Bivalvia. In: Kinne O (ed) Diseases of Marine Animals, Introduction, Bivalvia to Scaphopoda, Vol. II: 477-961; Biologische Anstalt Helgoland, Hamburg.

Lemanis R, Zachow S, Fusseis F, Hoffmann R (2015) A new approach using high-resolution computed tomography to test the buoyant properties of chambered cephalopod shells. Paleobiology 41: 313-329.

Lemanis R, Korn D, Zachow S, Rybacki E, Hoffmann R (2016) The evolution and development of cephalopod chambers and their shape. PLoS ONE 11(3): e0151404. doi:10.1371/journal.pone.0151404.

Leung TLF (2017) Fossils of parasites: what can the fossil record tell us about the evolution of parasitism? Biological Reviews 92: 410-430.

Littlewood DTJ, Donovan SK (2003) Fossil parasites: a case of identity. Geology Today 19: 136-142.

Longley WH (1930) Food of the Terns of the Dry Tortugas. Nature No. 3184: 737-739.

Longridge LM, Smith PL, Rawlings G, Klaptocz V (2009) The impact of asymmetries in the elements of the phragmocone of Early Jurassic ammonites. Palaeontologia Electronica 12.1.1A: 1-15.

Lukeneder A (2016) New size data on the enigmatic *Spirula spirula* (Decabrachia, suborder Spirulina), on a global geographic scale. In: Klug C, Hoffmann R, Fuchs D, Marty D (eds). Special Issue – Recent advances in Cambrian to modern cephalopod research II. Swiss Journal of Palaeontology 135: 87-99.

Lukeneder A, Harzhauser M, Müllegger S, Piller WE (2008): Stable isotopes (delta O-18 and delta C-13) in *Spirula spirula* shells from three major oceans indicate developmental changes paralleling depth distributions. Marine Biology 154: 175-182.

McLean N, Hochberg FG, Shinn GL (1987) Giant protistan parasites on the gills of cephalopods (Mollusca). Diseases of Aquatic Organisms 3: 119-125.

Mietchen D, Keupp H, Manz B, Volke F, (2005) Non-invasive diagnostics in fossils - Magnetic Resonance Imaging of pathological belemnites. Biogeosciences 2: 133-140.

Mietchen D, Aberhan M, Manz B, Hampe O, Mohr B, Neumann C, Volke F (2008) Three-dimensional magnetic resonance imaging of fossils across taxa. Biogeosciences 5: 25-41.

Mutvei H (1964) On the shells of *Nautilus* and *Spirula* with notes on the shell secretion in non-cephalopod molluscs. Arkiv för Zoologi 16: 221-278.

Mutvei H (2016) Siphuncular structure in the extant *Spirula* and in other coleoids (Cephalopoda). GFF 2016: 1-11.

Naef A (1922) Die fossilen Tintenfische-eine paläozoologische Monographie. Verlag Gustav Fischer, Jena 322 pp.

Naglik C, Monnet C, Goetz S, Kolb C, De Baets K, Tajika A, Klug C (2015) Growth trajectories of some major ammonoid sub-clades revealed by serial grinding tomography data. Lethaia 48: 29-46.

Neige P, Warnke K (2010) Just how many species of *Spirula* are there? A morphometric approach. In: Tanabe K, Shigeta Y, Sasaki T, Hirano H (eds) Cephalopods Present and Past, Tokyo, pp 77-84.

Nesis KN (1987) Cephalopods of the world. 1-351, T.F.H. Publications, Inc., Ltd.,, Food Industry Publishing House, Moscow.

Nikolaeva SV (2015) The type series of *Nautilus pompilius* Linnaeus, 1758 and *Spirula spirula* (Linnaeus, 1758). PIN RAN 2015: 49-51.

Nixon M, Dilly PN (1977) Sucker surfaces and prey capture. Symposia of the Zoological Society of London 38: 447-511.

Nixon M, Young JZ (2003) The brains and lives of cephalopods. Oxford University Press.

Ohkouchi N, Tsuda R, Chikaraishi Y, Tanabe K (2013) A preliminary estimate of the trophic position of the deep-water ram´s horn squid *Spirula spirula* based on the nitrogen isotopic composition of amino acids. Marine Biology 160: 773-779.

Okutani T, Suzuki K (1975) Concurrence of bathypelagic *Spirula spirula* and epipelagic *Argonauta boettgeri* in stomach contents of a Yellowfin Tuna from the Indian Ocean. Japanese Journal of Malacology (Venus) 34: 49-51.

Ozanne CR, Harries PJ (2002) Role of predation and parasitism in the extinction of the inoceramid bivalves: an evaluation. Lethaia 35: 1-19.

Pascual S, Gestal C, Estévez JM, Rodríguez H, Soto M, Abollo E, Arias C (1996) Parasites in commercially-exploited cephalopods (Mollusca, Cephalopoda) in Spain: an updated perspective. Aquaculture 142: 1-10.

Pascual S, González A, Guerra A (2007) Parasites and cephalopod fisheries uncertainty: towards a waterfall understanding. Rev. Fish. Biol. Fisheries 17: 139-144.

Pinhasi R, Mays S (2007) Advances in human palaeopathology, Wiley, New York.

Prell H (1921) Über die Schale von *Spirula* und ihren Verwandten. Centralblatt für Mineralogie, Geologie und Paläontologie 72: 183-190.

Price GD, Twitchett RJ, Smale C, Marks V (2009) Isotopic Analysis of the Life History of the enigmatic Squid *Spirula spirula*, with implications for studies of fossil cephalopods. Palaios 24: 273-279.

Priede IG (2017) Deep-Sea fishes – Biology, Diversity, Ecology and Fisheries. Cambridge University Press.

Ritterbush KA, Hoffmann R, Lukeneder A, De Baets K (2014) Pelagic palaeoecology: the importance of recent constraints on ammonoid palaeobiology and life history. Journal of Zoology 292: 229-241.

Ropolo P (1995) Implications of variation in coiling in some Hauterivian (Lower Cretaceous) heteromorph ammonites from the Vocontian basin, France. Memorie Descritive della Carta Geologica d'Italia 51: 137-165.

Sanchez, G., Setiamarga, D.H.E., Tuanapaya, S., Tongtherm, K., Winkelmann, I.E., Schmidbaur, H., Umino, T., Albertin, C., Allcock, L., Perales-Raya, C., Gleadall, I., Strugnell, J.M., Simakov, O., Nabhitabhata, J. (2018) Genus-level phylogeny of cephalopods using molecular markers: current status and problematic areas. PeerJ 2018: 1-19, DOI: 10.7717/peerj.4331.

Santos RA, Haimovici M (2002) Cephalopods in the trophic relations off southern Brazil. Bulletin of Marine Science 71: 753-770.

Seilacher A, Gunji PY (1993) Morphogenetic countdowns in heteromorph shells. Neues Jahrbuch für Geologie und Paläontologie Abhandlungen 190: 237-265.

Souidenne D, Florent I, Dellinger M, Justine JL, Romdhane MS, Furuya H, Grellier P (2016) Diversity of apostome ciliates, *Chromidina* spp.(Oligohymenophorea, Opalinopsidae), parasites of cephalopods of the Mediterranean Sea. Parasite, 23: 1-12.

Stalling D, Westerhof M, Hege, H-C (2005) Amira: a Highly Interactive System for Visual Data Analysis. In: Charles D. Hansen and Chris R. Johnson (eds.), The Visualization Handbook, pp. 749-767, Elsevier.

Stilkerich J, Smrecak TA, De Baets K (2017) 3D-Analysis of a non-planispiral ammonoid from the Hunsrück Slate: natural or pathological variation? PeerJ 5: e3526, https://doi.org/10.7717/peerj.3526.

Tajika A, Naglik C, Morimoto N, Pascual-Cebrian E, Hennhöfer DK, Klug C (2015) Empirical 3D-model of the conch of the Middle Jurassic ammonite microconch *Normannites*, its buoyancy, the physical effects of its mature modifications and speculations on their function. Historical Biology, 27: 181-191.

Tasnadi-Kubacska A (1962) Paläopathologie - Pathologie der vorzeitlichen Tiere. Gustav Fischer Verlag, Jena.

Tsujino Y, Shigeta Y (2012) Biological response to experimental damage of the phragmocone and siphuncle in *Nautilus pompilius* Linnaeus. Lethaia 45: 443-449.

Vinn O, Wilson MA, Toom U (2014) Earliest rhynchonelliform brachiopod parasite from the Late Ordovician of northern Estonia (Baltica). Palaeogeography, Palaeoclimatology, Palaeoecology 411: 42-45.

Ward PD (1982) The relationship of siphuncle size to emptying rates in chambered cephalopods: Implications for cephalopod Paleobiology. Paleobiology 8: 426-433.

Ward PD (1987) The Natural History of *Nautilus*. Allen & Unwin, Boston.

Ward PD, Boletzky Sv (1984) Shell implosion depth and implosion morphologies in three species of *Sepia* (Cephalopoda) from the Mediterranean Sea. Journal of Marine Biol. Association, U.K. 64: 955-966.

Warnke K (2007) On the species status of *Spirula spirula* (Linné, 1758) (Cephalopoda): A new approach based on divergence of amino acid sequences between the Canaries and New Caledonia. In: Landman NH et al. (eds) Cephalopods Present and Past: New Insights and Fresh Perspectives, Springer, pp 144-155.

Warnke K, Keupp H (2005) *Spirula* - a window to the embryonic development of ammonoids? Morphological and molecular indications for a palaeontological hypothesis. Facies 51: 65-70.

Warnke K, Oppelt A, Hoffmann R (2010) Stable isotopes during ontogeny of *Spirula* and derived hatching temperatures. Ferrantia 59: 191-201.

Yamaguchi A, Kumada Y, Alfaro AC, Wani R (2015) Abrupt changes in distance between succeeding septa at the hatchling time in modern coleoids *Sepiella japonica* and *Spirula spirula*. In: Klug C, Hoffmann R, Fuchs D, Marty D (eds)

Special Issue – Recent advances in Cambrian to modern cephalopod research I. Swiss Journal of Palaeontology 134, 301-307.

Young JZ (1977) Brain, behaviour and evolution of cephalopods. Symposia of the Zoological Society of London 38: 377-434.

Fig. 1 Median section (left) and cross section (right) of a *Spirula spirula* shell with conch dimensions used to calculate conch proportions and expansion rates (ASI_{20} circle not to scale).
Single column, b/w in print, colour in pdf

Fig. 2 Overview of the four *Spirula spirula* shells that have been analysed in order to quantify their 2D shape changes during ontogeny as well as volumetric trajectories. **A-D** lateral surface view of the shells, arrows in **B** and **D** indicate CT-artefacts due to the marginal position of the shells in the cone beam during scanning not shell pathologies, note: boxes in **B-D** indicate areas of pathologies, box in **A** indicate changes in shell shape assigned to the terminal countdown morphology sensu Seilacher and Gunji (1993), **E-H** virtual median sections, **I-L** visualization of the chamber volumes only, with each chamber volume in a different colour; **A, E, I** a normal (non-pathological) shell from the Maldives (coll. no.: 2015/0022/0001); **B, F, J** one shell found at the beach of Fuerteventura with crushed chambers 15 (coll. no.: RUB-Pal 11250); **C, G, K** shell collected in West-Australia with malformed chambers six (fifth preserved) (coll. no.: 2015/0020/0007), **D, H, L** another shell from Fuerteventura with one unusual thick septum (coll. no.: RUB-Pal 11255); scale bar = 5 mm.
double column, b/w in print, colour in pdf

Fig. 3 Close ups of the areas indicated with boxes in Fig. 2. **A-C** Shell from the Maldives (coll. no.: 2015/0022/0001) with the terminal countdown morphology characteristic for the adult stage of *Spirula* including vanishing shell surface ornamentation (**A-B**) and septal crowding (**C**). **D-F** Shell from Fuerteventura (coll. no.: RUB-Pal 11250) with crushed chamber 15 with significantly reduced whorl height (**D-E**) and remnants of shell material in the chamber (**F**). **G-I** Shell from West-Australia (coll. no.: 2015/0020/0007) with crushed chamber six (fifth preserved) (**G-H**, arrow) and an overall elliptical shell shape and remnants of shell material in chamber six (**I**, arrow). **J-L** Shell from Fuerteventura (coll. no.: RUB-Pal 11255) with a single thickened septum (**L**) note the absence of shell ornamentation (arrow; see **Fig. 2** for scale).
double column, b/w in print, b/w in pdf

Fig. 4 *Spirula spirula* shell (BSPG 2014 XXI 88005) with a blister. **A-B** left and right lateral view, **C** median section with a star indicating the position of the blister, box (D) marks the field of view. **D** close up to show the blister and its opening (arrow), note the absence of surface crenulation, **E** view from the inside of the chamber showing a larger opening of the blister on this side (compare with **F-I**), **F-I** cross sections cutting through the blister at different positions showing the relatively large opening towards the chamber and the small opening at the external shell layer, **J** chamber volume with the associated volume of the

blister (arrow) in blue-green, **K** translucent shell with the connecting strand in the middle (siphuncle) and the chamber with blister in blue-green.
double column, b/w in print, colour in pdf

Fig. 5 *Spirula spirula* shell (BSPG 2014 XXI 88006) with a callus at the aperture. **A-B** left and right lateral view, arrows in **B** show shell fragments that have been covered with additional shell layers after a predator attack, **C** median section reveals the significant thickening of the four preserved septa, the siphuncle however is in place but with shorter septal necks, **D** septal surface with the siphuncle (arrow) and an irregular shaped area, **E** close up of the irregular shaped area showing additional shell material, **F** cross section through the whorl at about the area shown in **E**, septa are irregularly shaped, significantly thicker and partly with a rough surface but most significantly the septa leave a small non-mineralized area open connecting four chambers, **G-J** cross section revealing the irregular mineralization of the septa.

double column, b/w in print, b/w in pdf

Fig. 6 *Spirula spirula* shell (BSPG 2014 XXI 88007) with a callus at the aperture. **A-B** left and right lateral view **C** median section, **D** close up refers to box in **A** showing the external shell surface with the irregular callus covered with weak striae and small spherulitic structures **E** irregularly shaped septal surface also affected by the callus formation, F close up refers to box in **C**, not the irregular mineralization of the septum and conch wall composed of several layers, and the dislocated siphuncle, G-J whorl cross section documenting the alternating mineralized and non-mineralized layers with small spherulitic structures.
double column, b/w in print, b/w in pdf

Fig. 7 *Spirula spirula* shell (SNSB-BSPG 2018 I 21) **A-B** left and right lateral view, arrow in **B** point to the non-lethal injury, **C** apertural view, **D** median section, white box indicates a slight thickening of the conch wall, **E-H** close ups of the whorl cross section, showing shell fragments re-incorporated in the conch wall after a predator attack.
double column, b/w in print, b/w in pdf

Fig. 8 *Spirula spirula* shell (SNSB-BSPG 2018 I 22) **A-B** left and right lateral view, arrow in **B** point to the non-lethal injury, **C** apertural view, **D** median section, white box – area of injury with a thick septum, material of the conch wall hanging within the chamber and decreased whorl height, **E-G** close ups of the injured area with **E** whorl cross section showing shell fragments re-incorporated in the conch wall after a predator attack **F** median section showing a decreased siphuncle diameter and a shell thickening (arrow), **G** median section showing the thick septum and old conch wall material piercing into the chamber (arrow), note that also the conch wall is thicker over the length of one chamber.
double column, b/w in print, b/w in pdf

Fig. 9 Ontogenetic trajectories for different 2D shell parameters **A** whorl width index (WWI) **B** whorl interspace index (WII) **C** whorl expansion rate (WER) **D** umbilical width index

(UWI) **E** septa per demi-whorl (SDW), dotted line indicates ontogenetic trajectories for the "normal" shell from the Maldives.

1.5 column, b/w in print, b/w in pdf

Fig. 10 Ontogenetic trajectories for different 3D and angular shell parameters, **A** chamber volume with an inserted graph **A1** for the first 15 chambers, **B** total chamber volume and total rotational angle, **C** difference in chamber volume of succeeding chambers with an inserted graph **C1** for the first 15 chambers, **D** inner chamber surface area with an inserted graph **D1** for the first 15 chambers.

1.5 column, b/w in print, b/w in pdf

Fig. 11 Ontogenetic trajectories for different 3D and angular shell parameters, **A** differences of inner chamber surface area of succeeding chambers, **B** chamber volume against chamber surface **C** Vogel number graph, **D** septal angle **E** differences in septal angle of succeeding septa (note that in **D-E** the earliest chambers are cut off see **Supp. Fig. 4** for a complete graph).

1.5 column, b/w in print, b/w in pdf

Fig. 12 Live caught *Spirula spirula* specimen (leg. K. Warnke) from the Canary Islands, **A** ventral view, arrow shows the funnel, **B** dorsal view, **C** volume rendering, arrows points to a gill branch, light yellow = shell and statoliths, **D** surface rendering of the shell and the statoliths.

double column, b/w in print, colour in pdf

Supplementary Figures

Supp. Fig. 1 *Spirula spirula* shell (RUB-Pal 11255) with a single septum that is significantly thicker compared to preceding and succeeding septa, **A** original shell with eight additional chambers preserved, dm = 20.4 mm **B** median section, close up of the interconnection between septa and conch wall, arrows indicate different grayscale values for the septa permitting identification of their insertion into the conch wall, potentially the gray scale values are due to different amounts of organic material within the mineral layers rendering the septa less dense **C** external shell surface at about the position with the thick septum (arrow) resulting a small lateral bulges **D** internal view of that same area (arrow with black frame), each chamber nicely shows the muscle attachment scar (white arrow), **E** whorl cross section showing a blister-like structure sitting in the conch wall (arrow) **F** same area seen in an orthoslice with different greyscale for the septal material and the conch wall **G-H** close ups of the insertion area between septum and conch wall clearly showing were the septum ends and that the blister-like structure was filled with conch wall material that was broken off (arrow in **G**)

Supp. Fig. 2 *Spirula spirula* shell (RUB-Pal 11250) showing close ups of the crushed chamber with additional shell material sealing off the chamber **A** median section out of the centre also showing the siphuncle and a shell fragment in the upper part of the chamber **B** close up showing the siphuncle with a somewhat crinkled appearance **C** siphuncle of the

succeeding chamber showing a weak bulge towards the crushed chamber not seen in any other *Spirula* septal neck and accordingly part of the reaction to the prior injury **D** close up of the additionally precipitated shell material showing its spherulitic appearance

Supp. Fig. 3 Additional ontogenetic trajectories for different 2D shell parameters **A** whorl height expansion rate (WHER) **B** whorl width expansion rate **C** conch height index (CHI) **D** conch width index (CWI)

Supp. Fig. 4 Additional ontogenetic trajectories for angular measurements **A** absolute septal index for a circle of 20 mm in diameter (ASI_{20}) B septal angle for all chambers **C** difference in angular measurements between succeeding septa

Table 1 Collection numbers, Location, pathology, maximum diameter, number of preserved chambers, voxel size, and acquired data size for every specimen used in this study.

Specimen	Locality	pathology	dm_{max} in mm	Number of preserved chambers	Voxel size in µm	Data size in GB
2015/0022/0001	Maldives	none	25.8	37	9.8	17.9
RUB-Pal 11250	Fuerteventura	crushed chamber	18.65	39	8.3	10.9
same		close up			5.0	14.2
RUB-Pal 11255	Fuerteventura	thickened septum	14.94 (20.4)	27 (35)	8.3	7.4
same		close up			5.0	14.2
RUB-Pal 11249 (see Hoffmann et al. 2015a)	Fuerteventura	?anomal chamber volumes	17.55	30	8.7	14.4
2015/0020/0007	W-Australia	pathological earliest chambers	17.86	38	8.6	8.1
SHK PC-5 BSPG 2014 XXI 88005	Gran Canaria	blister	17.5	21	7.5	8.5

SHK PC-6 BSPG 2014 XXI 88006	Gran Canaria	callus	7 mm fragment	36	7.5	7.5
SHK PC-7 BSPG 2014 XXI 88007	Gran Canaria	callus	17.5	22		
same		close up			5.5	30.5
SNSB-BSPG 2018 I 21	Gran Canaria	lateral injury	16.16	29	8.0	6.9
SNSB-BSPG 2018 I 22	Gran Canaria	lateral injury	12.66	14	7.0	6.3
Spirula live caught specimen	Canary Island	none	13.67	26	6.2	86.6

Table 2 Calculated buoyancy value for the pathological *Spirula* shells shown in Fig. 2.

Specimen	Shell Volume (m^3)	Total Weight (N)	Buoyancy (N)	Buoyancy Difference between pathologic and non-pathologic shells
RUB-Pal 11250	7.46701E-09	0.00579024	-8.01323E-05	7.41661E-05
2015/0020/0007	9.66083E-10	0.000534904	-1.36116E-05	5.53529E-06
RUB-Pal 11255	5.83315E-08	0.030798518	0.000701484	0.000141902

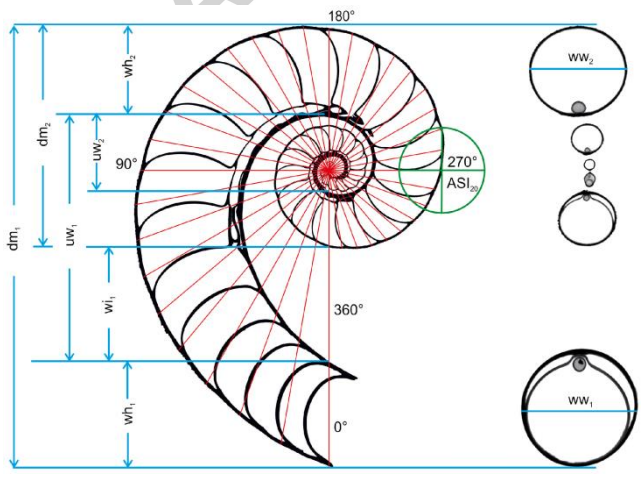

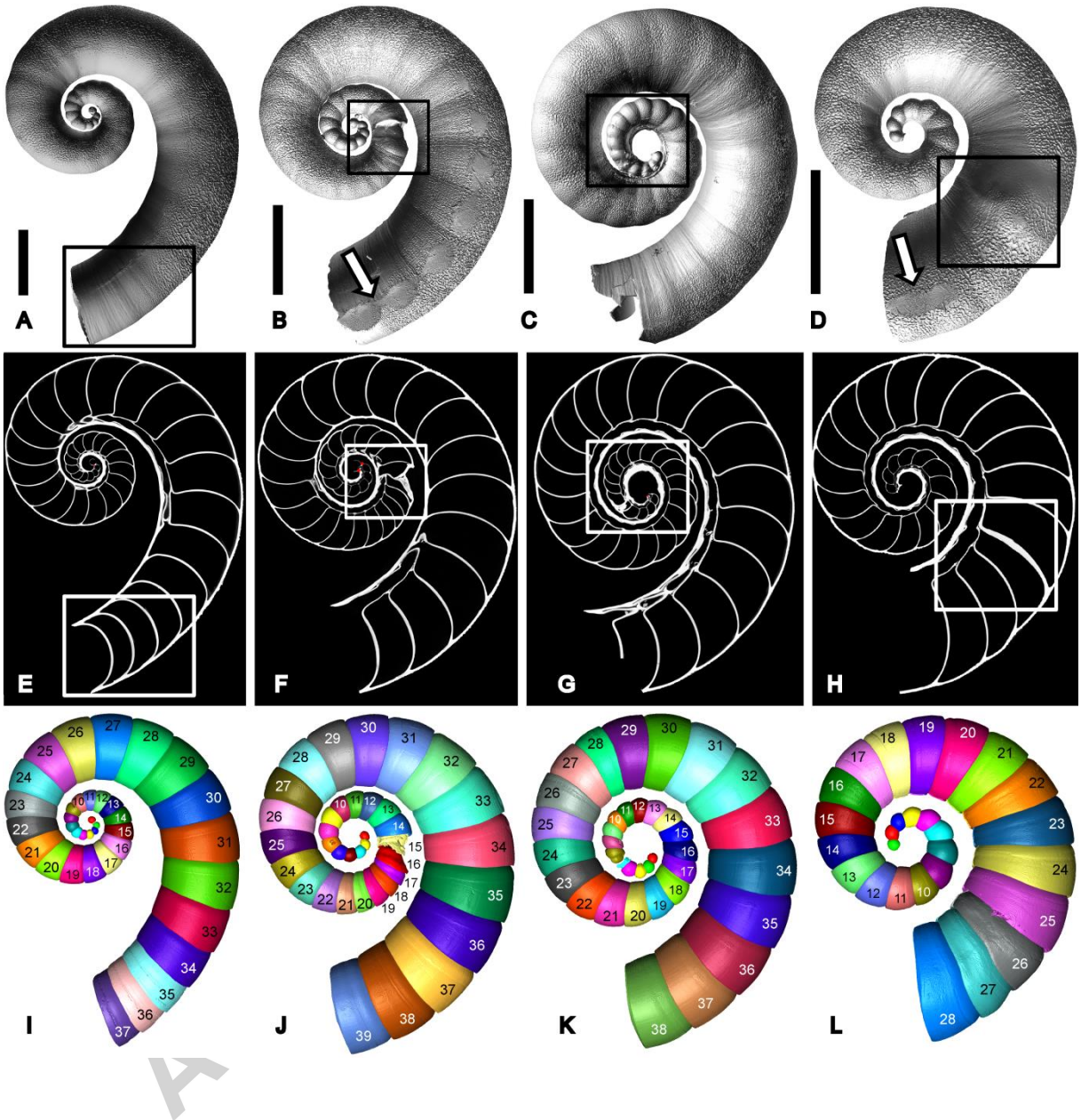
A
B
C
D
E
F
G
H
I
J
K
L

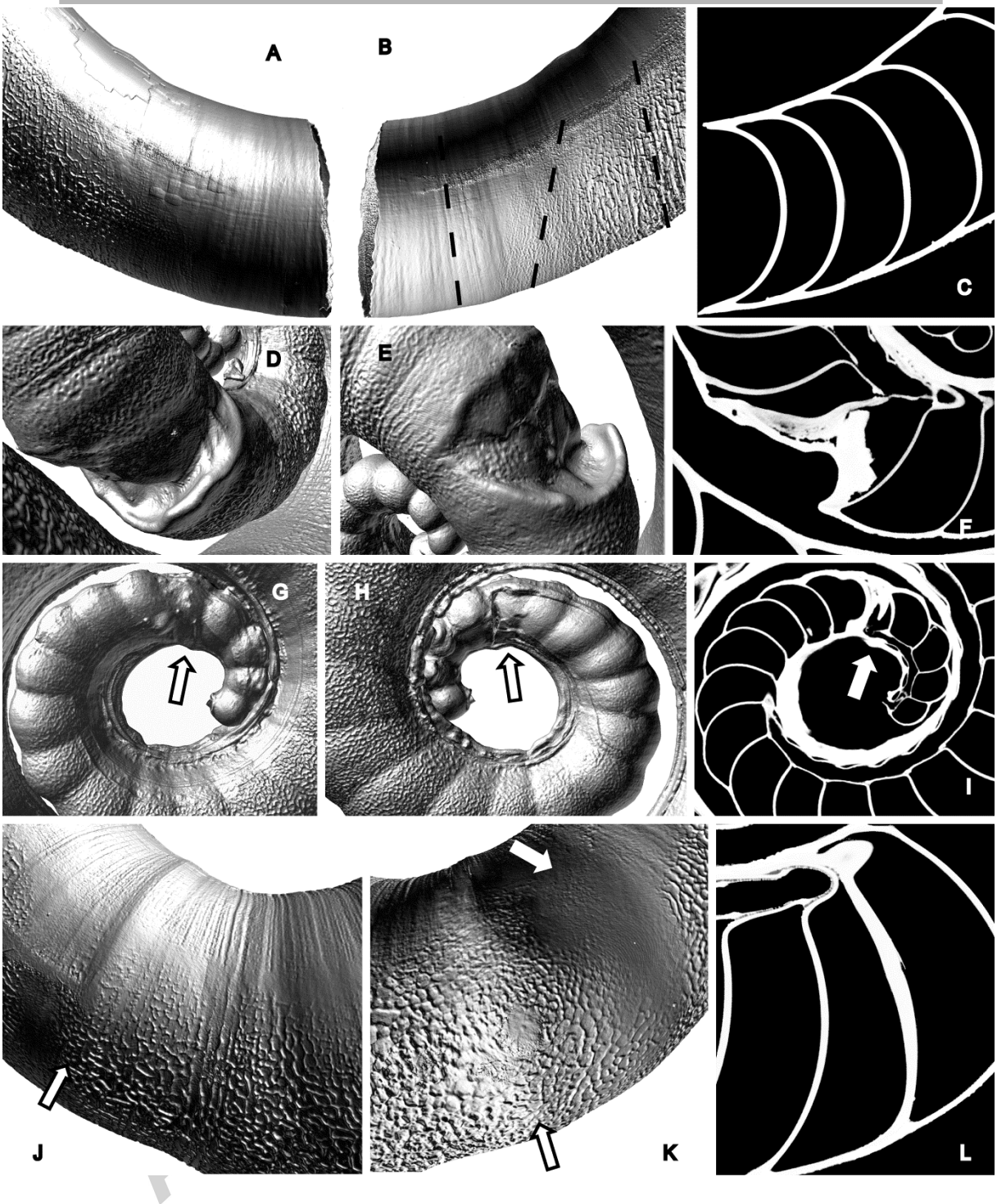

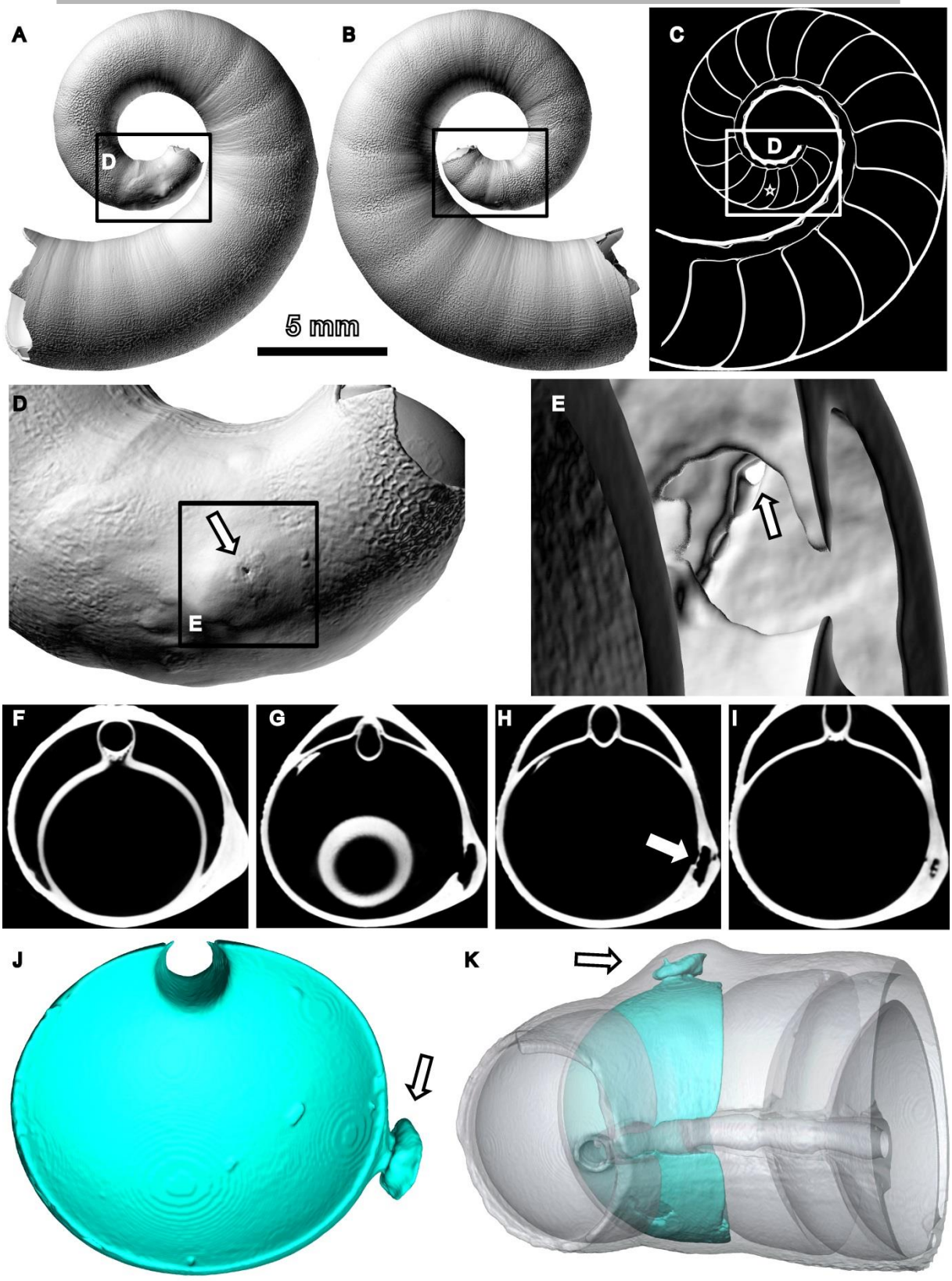

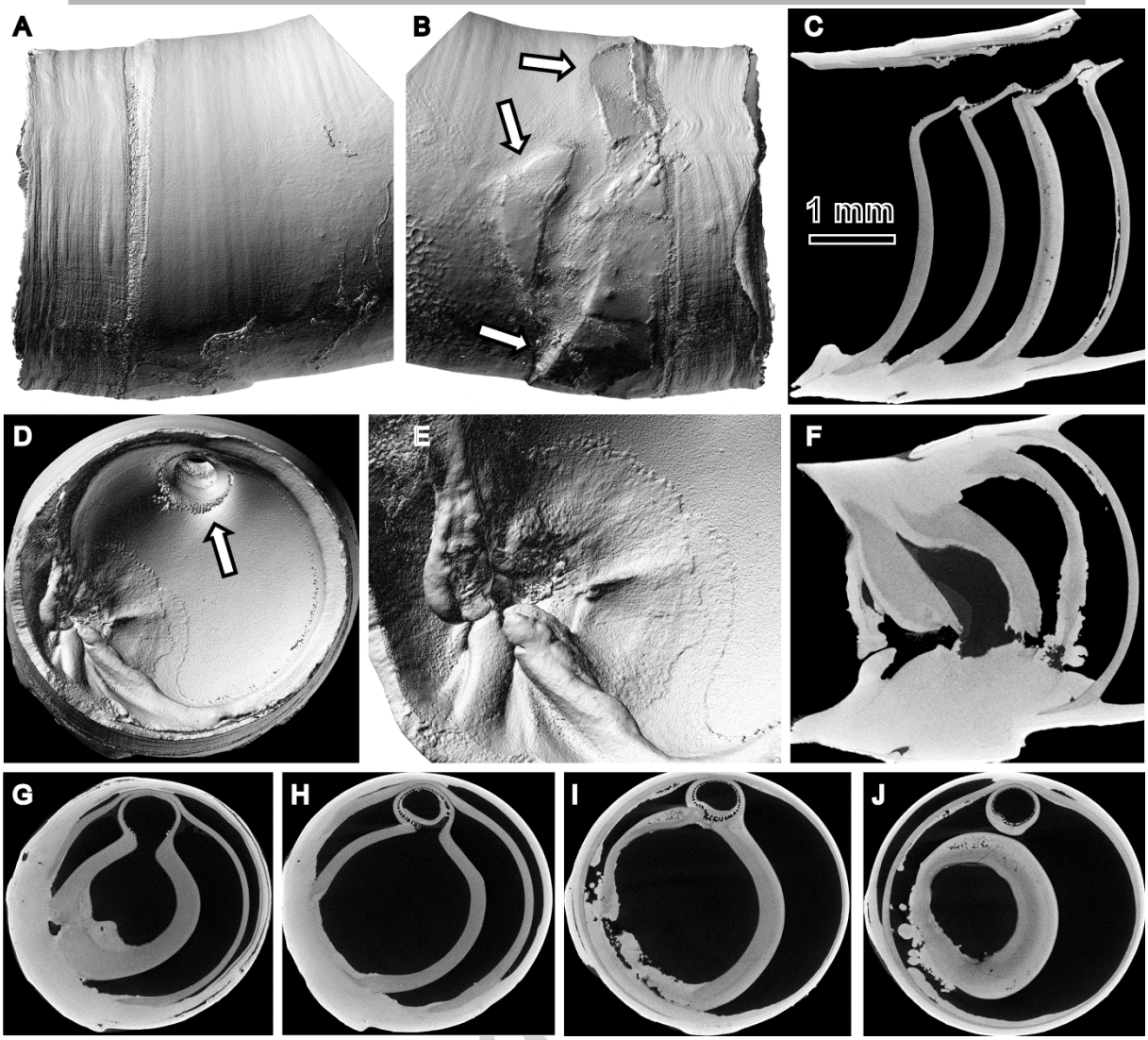

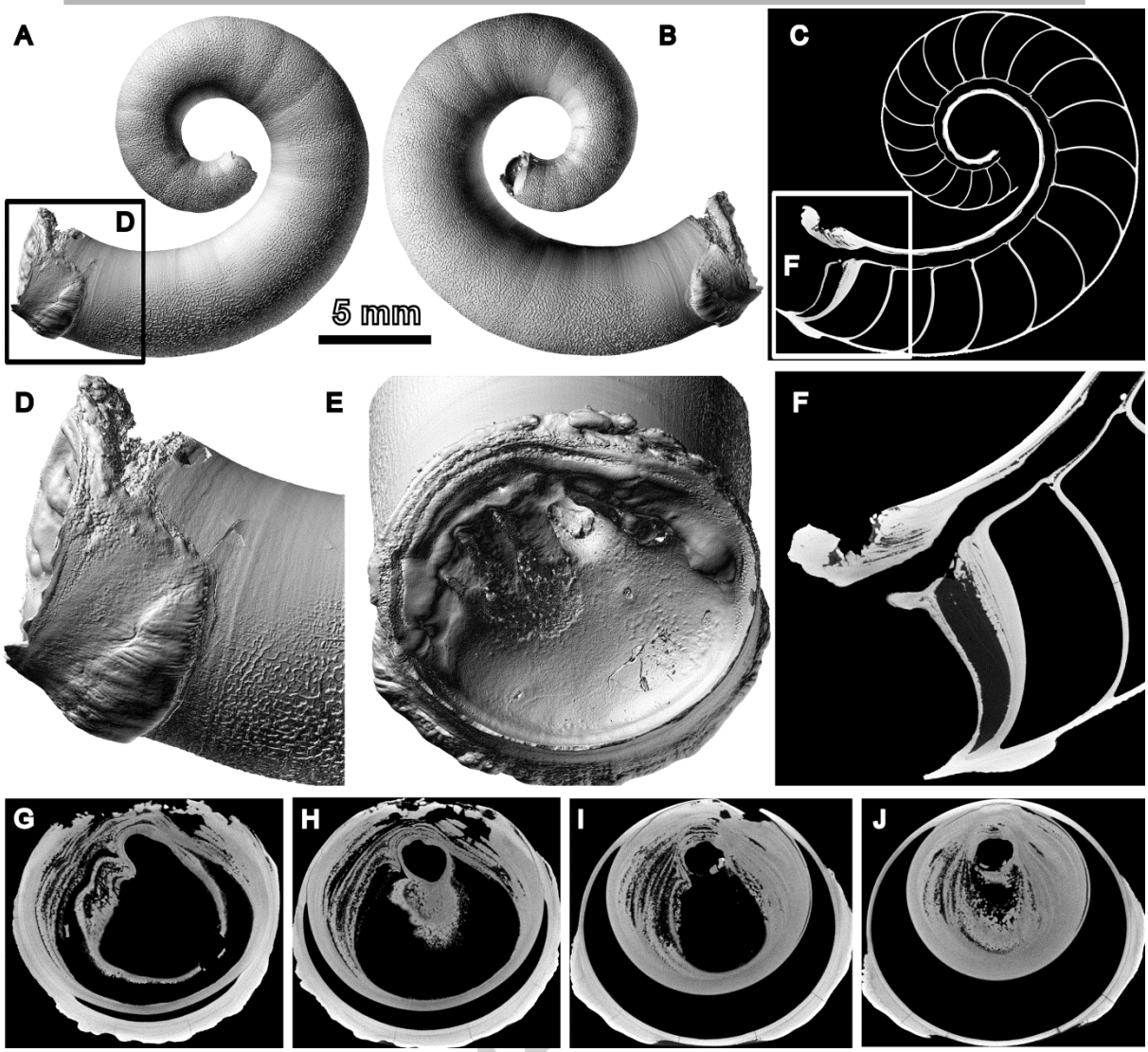

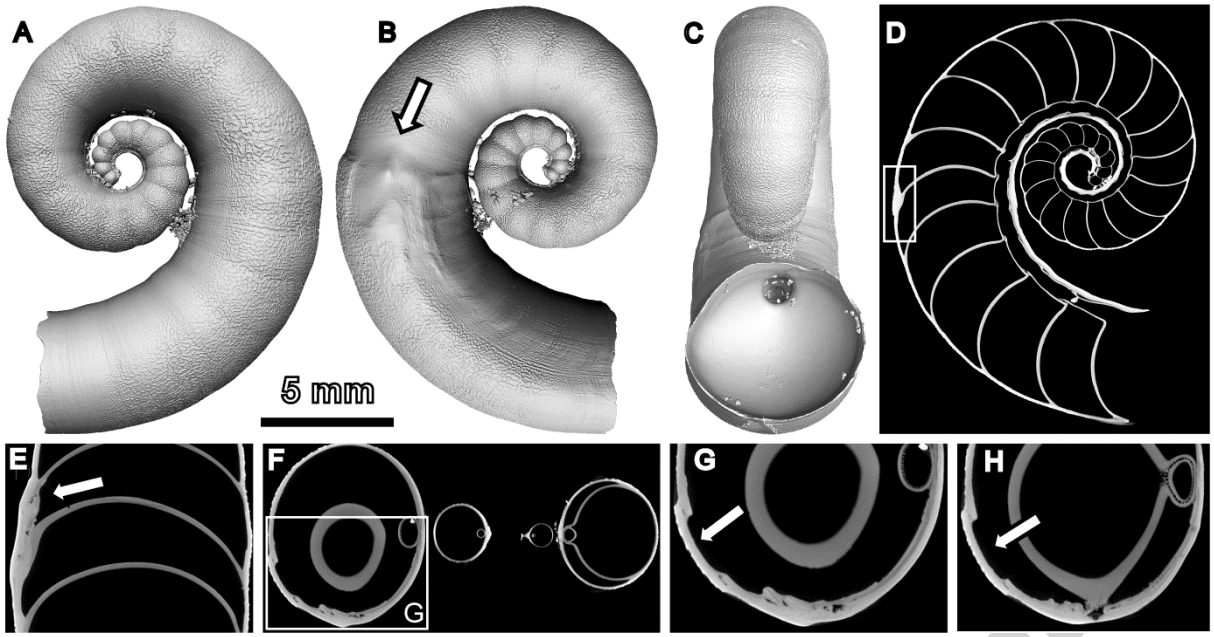
A
B
C
D
5 mm
E
F
G
H
G

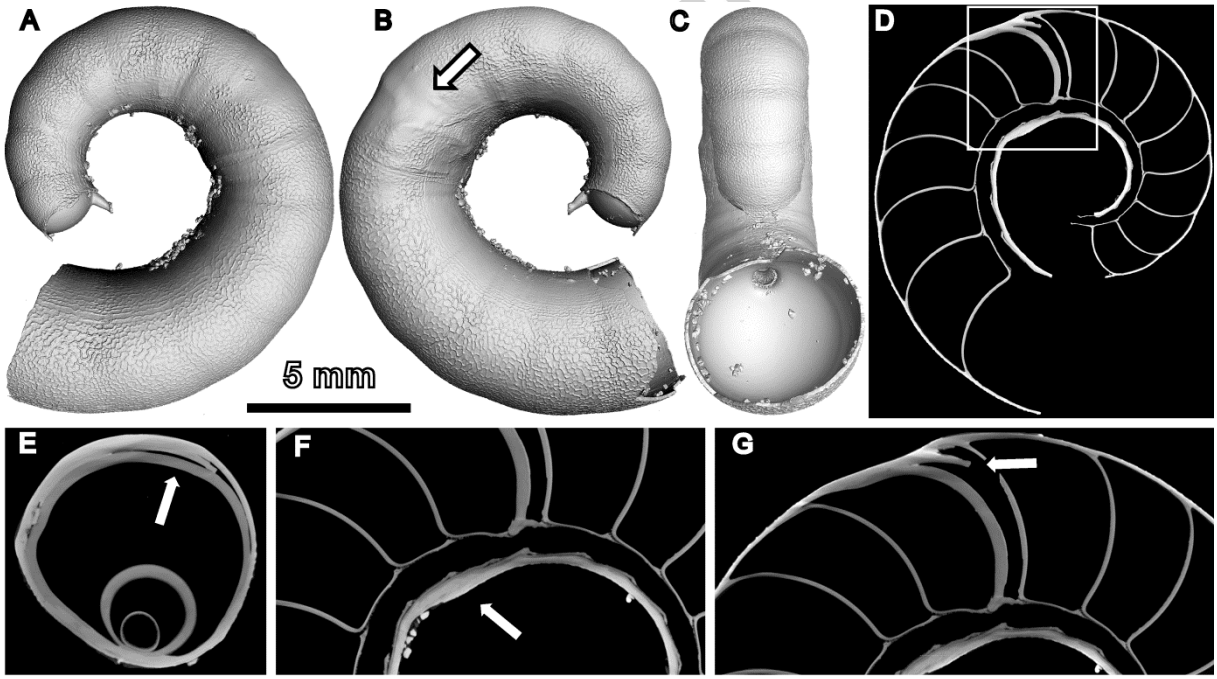
A
B
C
D
5 mm
E
F
G

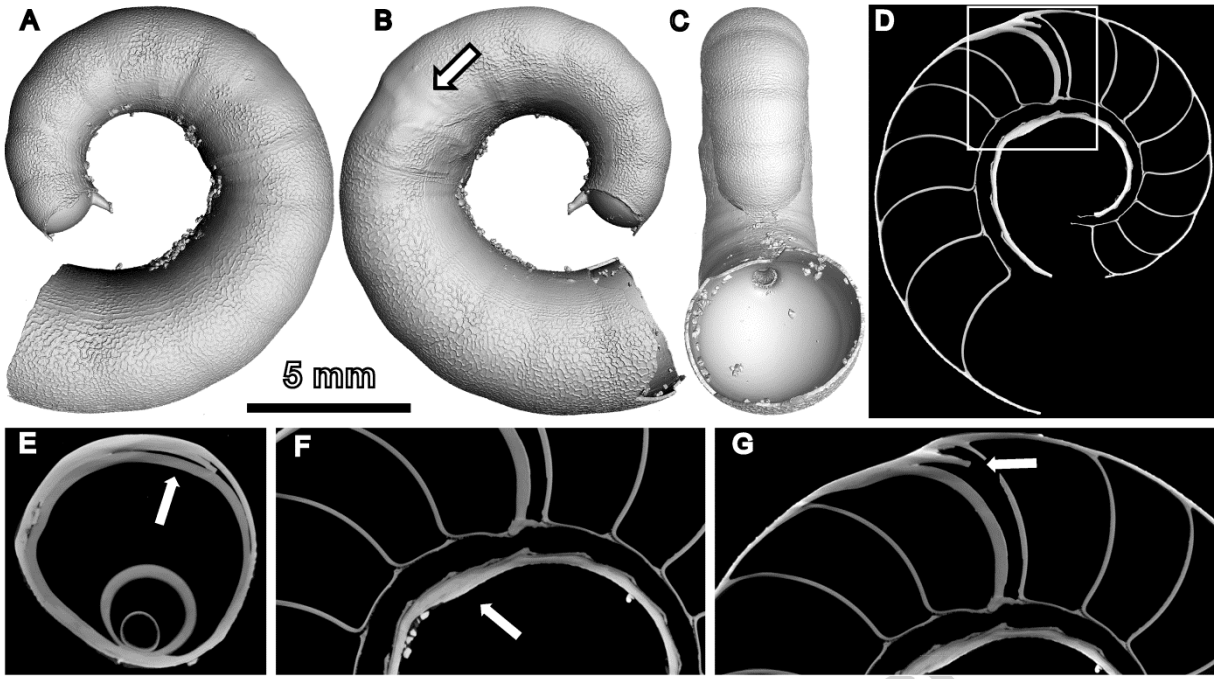

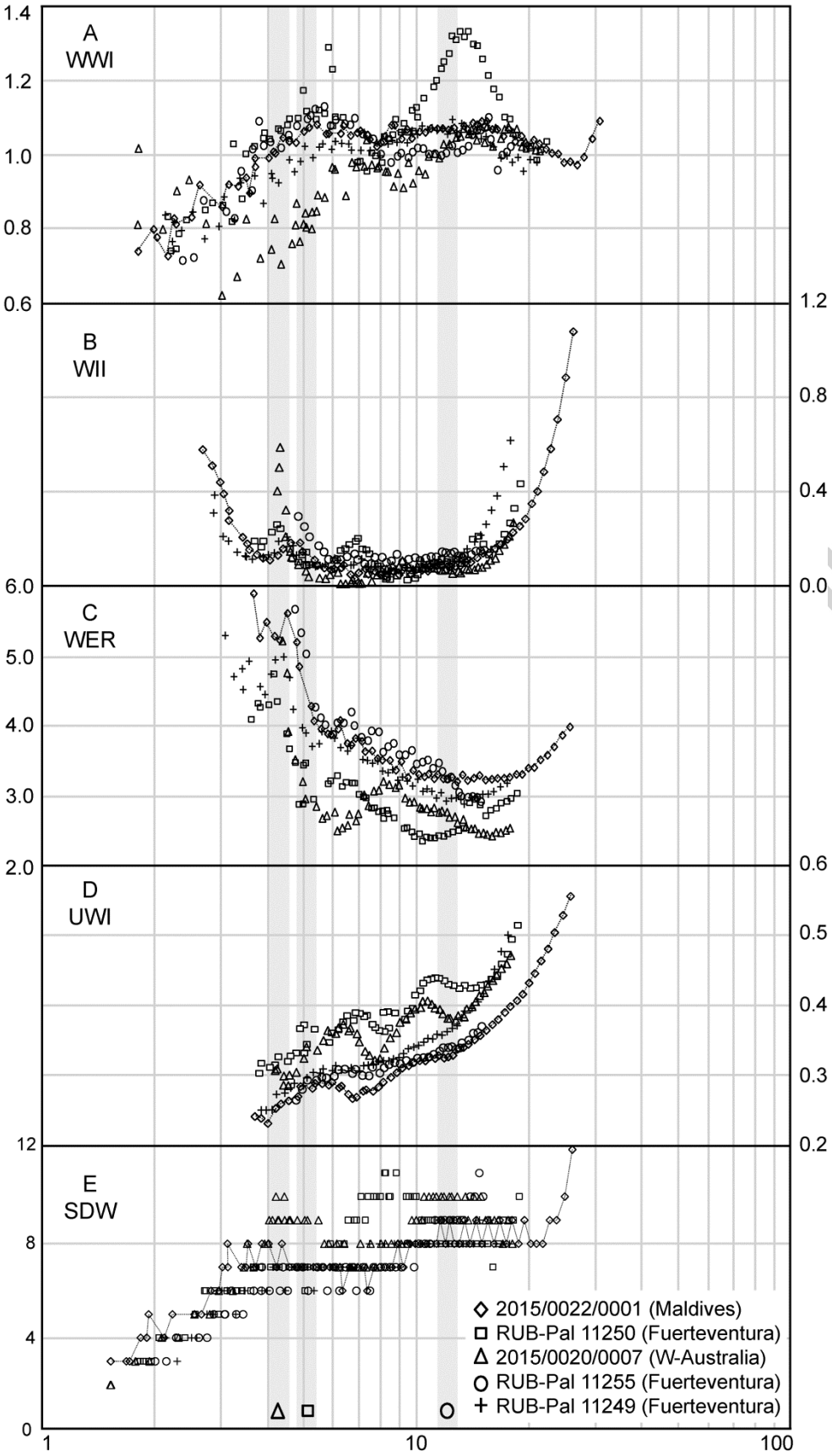

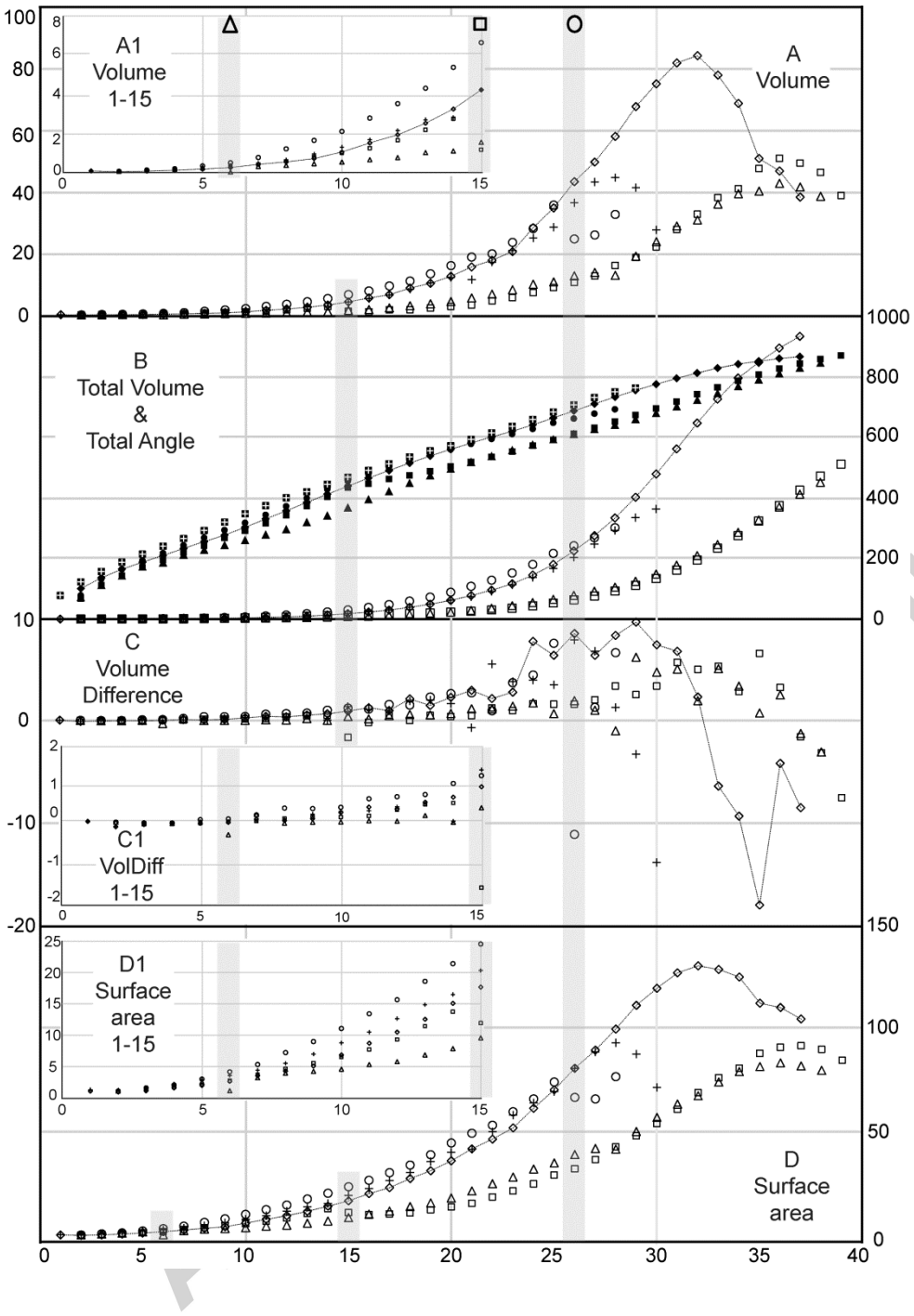
A1
Volume
1-15
A
Volume
B
Total Volume
&
Total Angle
C
Volume
Difference
C1
VolDiff
1-15
D1
Surface
area
1-15
D
Surface
area